Time-Switching EH-Based Joint Relay Selection and Resource Allocation Algorithms for Multi-User Multi-Carrier AF Relay Networks

Ankit Gupta, Keshav Singh, *Member, IEEE*, and Mathini Sellathurai, *Senior Member, IEEE*

***Abstract*—In this paper, an energy efficiency maximization (EEM) optimization problem for the multi-user multi-carrier energy-constrained amplify-and-forward (AF) multi-relay network is formulated under the total source transmit power budget and energy-causality constraints. We consider that each relay node is solely powered by the source nodes, employing energy harvesting time-switching (EHTS) protocol to harvest the energy through the ambient radio-frequency (RF) signal transmitted from the source nodes under the simultaneous wireless information and power transfer (SWIPT) paradigm. First, we propose a subcarrier and energy causality-based multi-relay selection policy. Second, we jointly optimize the parameters that control the energy efficiency (EE) of the system namely multi-relay selection, subcarrier pairing, user allocation, power allocation, and RF EHTS time block, that renders the problem to be a mixed integer non-linear programming problem (MINLP) which remains NP-hard to solve. Hence, we remodel the problem to a tractable quasi-concave form by applying a string of convex transformations. Later, we propose an iterative EEM algorithm to optimize the multi-parameter problem. Further, a suboptimal and best relay selection algorithm is studied by trading-off between complexity and performance. The effectiveness of the proposed algorithms is demonstrated by simulation results.**

***Index Terms*—Energy efficiency, resource allocation, multi-user, amplify-and-forward, relay selection, SWIPT, RF energy harvesting, time-switching protocol.**

I. Introduction

With the advent of Internet-of-things (IoT) communication networks, and widespread applications of small devices, such as in sensor nodes, has led to tremendous growth in data-rate requirements, the biggest challenge faced for the practical realization of these dense IoT networks is constant power supply. Therefore, to meet these requirements it is currently projected that by the end of 2030, there will be about 4 Gt (Gigatonnes) of CO_2 emissions by the information and communication (ICT) sector [1]. To achieve the green-target for the environment, one effective way is to harvest energy from the ambient sources like solar, wind etc [2], [3] or radio-frequency (RF) signals. Another way is to design cellular networks with greater scrutiny towards energy-aware engineering and resource allocation policies that not only prolong the network's lifespan, but also contribute towards energy savings under the protection of green communications [1]. Thereby, developing an energy-efficient energy harvesting (EH) network, will not only provide notable positive impacts on the environment, but also long-term profitability to the ICT operators.

In contrast to the time, location and weather dependent conventional EH methods, simultaneous wireless information and power transfer (SWIPT) has emerged as a paradigm substitute to the traditional power supply, especially for energy-constrained battery-powered devices [4]. In a SWIPT network, the receiver node is allowed to harvest energy from the received RF signal, thereby achieving the trade-off between information forwarding (IF) and EH. However, SWIPT RF EH suffers from a disadvantage of communication over long distances, as the received power fades exponentially [5]. In the cooperative communication network, the nodes are generally powered by utilizing the pre-charged batteries or with power-grid, but both of these power-supply sources faces practical challenges and are uneconomical in nature. Therefore, cooperative communications and SWIPT technique can benefit one another by overcoming the drawbacks of the other, such as, SWIPT technique can provide the relay nodes with the required power for its operation in exchange of ubiquitous coverage, augmented throughput and ameliorated link dependability [6]. Moreover, the amplify-and-forward (AF) relaying is widely preferred over decode-and-forward (DF) relaying due to its lower implementation complexity [7], [8].

Fundamentally, the SWIPT relaying protocols [4] are broadly classified as EH time-switching (EHTS) [9] and EH power-splitting (EHPS) [10] protocol. In EHTS relaying protocol the relay node dedicates particular time slot for EH and IF for the signals received from RF source nodes. Firstly, by employing the EHTS protocol, we can directly utilize the off-the-shelf commercially available circuits, which have been designed for separate functionalities of energy harvesting and information decoding, thereby reducing the receiver complexity as compared to EHPS protocol. Secondly, the power

Manuscript received September 15, 2018; revised January 10, 2019; accepted March 11, 2019. Date of publication March 20, 2019; date of current version May 16, 2019. This work was supported in part by the U.K. Engineering and Physical Sciences Research Council under Grant EP/P009670/1, and in part by the U.K.-India Education and Research Initiative Thematic Partnerships under Grant UGCUKIERI 2016-17-058. The associate editor coordinating the review of this paper and approving it for publication was L. Wang. *(Corresponding author: Mathini Sellathurai.)*

A. Gupta and M. Sellathurai are with the Signal Processing for Intelligent Systems and Communications Research Group, Heriot Watt University, Edinburgh EH14 4AS, U.K. (e-mail: ag104@hw.ac.uk; m.sellathurai@hw.ac.uk).

K. Singh is with the Institute for Digital Communications, University of Edinburgh, Edinburgh EH9 3FG, U.K. (e-mail: k.singh@ed.ac.uk).

Digital Object Identifier 10.1109/TGCN.2019.2906616

splitter employed in EHPS protocol is an uncommon hardware, adding to the design complexity, thus EHTS protocol is widely employed for ease of deployment. Lastly, the EHTS utilizes the following facts to its advantage 1) the energy receiver and information receiver works under significantly different power sensitivity, for example the energy receiver usually works over 10 dBm whereas the range of the information receiver is -60 dBm; and 2) the wireless channels fluctuates in huge power ranges (e.g., tens of dBs) because of the time-varying channels and effects like shadowing, interference, path-loss etc. Hence, EHTS protocol can optimize its time-switching capabilities to its advantage. Therefore in this work, we utilize EHTS protocol for harvesting energy from the procured RF signal at the relay node.

A. Related Works

Recently RF energy based SWIPT technique has been studied for improving the spectral efficiency (SE) of the network for a single user pair in [9]–[14]. Guo and Zhou [15] considered an energy-efficient power allocation scheme for DF relaying by employing EHPS protocol. Li *et al.* [16] have considered a single user-pair and a single relay node with a single eavesdropper node, and maximized the achievable secrecy sum rate of the two-way relay network under the transmit power constraint at the relay and the EH constraint at the EH receiver by utilizing the sequential parametric convex approximation (SPCA) based iterative algorithm. However, the works [9]–[16] have considered a single-user pair scenario except [17] which does not consider relaying strategies. However, considering a multi-user scenario will be more practical and none of the above works have considered a multi-user pair scenario employing SWIPT protocol. In contrast to a single carrier transmissions, SWIPT was recently introduced with the well-established benefits of multi-carrier transmissions [18], [19]. Further, with the advancement of the automotive industry, we are currently moving towards the development of smart vehicles that will be safer, efficient, economical and greener, giving rise to intelligent transportation systems (ITS). The ICT will play a major role in the success of the ITS system [20]. For example, information and communication from road infrastructure-to-vehicle (I2V) performs a major part in management of traffic, assistance in driving and floating car data [21]. Recently, ITS has started to employ multi-source multi-relay vehicular communications because of the support provided by the wireless nodes present in road I2V [22], thereby increasing the link reliability, network coverage and connectivity through distributed spatial diversity [23]. However, power allocation strategies still remains the biggest challenge for the performance of these ITS network [24]. Moreover, many recent works have studied multi-user multi-relay scenario in ITS networks. Moreover, the works [9]–[19] did not consider a multi-carrier multi-user multi-relay scenario from the EE perspective with EHTS protocol, to the best of authors' knowledge. Therefore, the proposed multi-carrier model will bring additional advantages to the multi-user multi-relay network, but with additional challenges of resource allocation.

B. Motivation and Contributions

The aforementioned discussion motivates us to consider a multi-user multi-carrier EHTS AF multi-relay scenario with the aim of maximizing the EE of the network, subject to a total source transmit power budget and energy-causality constraints. However, multi-user, multi-carrier, AF relay network faces major difficulties such as the multi-relay selection strategy and allocation of the selected relays to user pairs and subcarriers, because of the exponential possible combinations for joint subcarrier pairing along with user allocation and multi-relay selection. In contrast to [18] and [19], we consider AF relaying in this work, herein we consider a multi-carrier based multi-user multi-relay networks. Therefore, the interference management and noise amplification are required to be addressed by the optimal resource allocation policy. Further, determining the optimal EHTS time block plays a pivotal role in balancing the EH and IF for each selected relay to maximize the EE for the limited EH network. Different from [18] wherein EHTS time block is obtained by searching between its determined lower-bound and upper-bound values, in this work we determine the optimal EHTS time block for each relay on each subcarrier, that present additional challenges. To overcome these problems, we propose a joint optimization of the parameters that control EE of the network: power allocation, EHTS time block, multi-relay selection, subcarrier pairing and user allocation. For reasons of clarity, we summarize the contributions of this paper as follows:

- In the first part of our joint optimization problem, we propose a multi-relay selection scheme wherein the model decides - *i*) number of cooperating relays, *ii*) user pairs allocated to the selected relays and *iii*) subcarrier allocation for selected relays, by considering the subcarrier pairing, user allocation and energy causality constraints. Herein, the energy causality constraint takes into account of the subcarrier pairing and relay's static power dissipation to model the relay selection policy and mandates that the relays with sufficient harvested energy and better channel conditions that maximise network's EE are only selected.
- For jointly optimising EHTS time block, subcarrier pairing permutation, multi-relay selection, subcarrier and power allocation we formulate the network's EE maximising optimization problem, subject to total source transmit power budget. It renders to a mixed integer nonlinear programming problem (MINLP), which remains NP-hard to solve [26]. Hence, we remodel the problem to a tractable quasi-concave form by applying a lower bound successive-convex approximation (SCA), similar to the SPCA applied in [16], along with variable transformations, introducing auxiliary variable [26] and Dinkelbach's method [27].
- Based on the dual decomposition [26], an iterative EE maximization (EEM) algorithm for EHTS protocol is proposed, wherein we first obtain the optimal subcarrier pairing, power allocation, multi-relay selection and subcarrier allocation and later we optimally determine the EHTS time block.

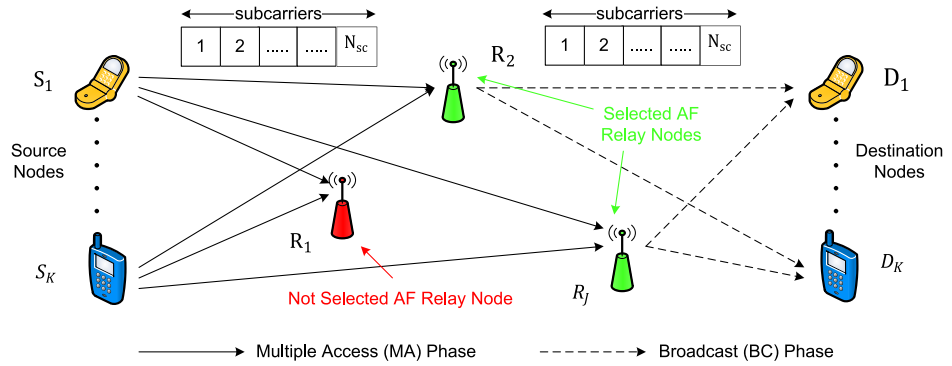

Fig. 1. Structure of multi-user energy-constrained AF EH relay-assisted network.

- The complexity of the proposed algorithms is further analysed. Furthermore, we investigate a suboptimal EEM algorithm, with curtailed complexity but tolerable performance deterioration. Moreover, we also study the joint resource allocation and best relay selection policy. The achievements of the suggested algorithms and the influence of numerous network parameters on the feasible EE and SE are manifested via computer simulations.

The remainder of the paper is as follows. In Section II, we describe the system model, introduce the power dissipation, EE, multi-relay selection and energy causality model. The problem formulation and its transformation to a convex form are described in Section III. The proposed iterative resource allocation algorithm is presented in Section IV. The suboptimal resource allocation algorithm and best relay resource allocation algorithm are investigated in Section V. The complexity analysis is illustrated in Section VI, followed by the simulation results in Section VII. Conclusions and future works are depicted in Section VIII.

II. System Model

Consider an energy-constrained AF multi-relay cooperative network as illustrated in Fig. 1, consisting of K source-destination pairs $(S_k - D_k)$, for, $k \in \{1, \ldots, K\}$, and J intermediary relay nodes R_j, for $j \in \{1, \ldots, J\}$, whilst N_{sc} subcarriers are available for transmission in each hop. Each node operates with a single antenna in half-duplex mode, i.e., it cannot transmit and receive concurrently, as endured in sensor networks [28]. Each user[1] node has a conventional energy supply, whereas each relay node solely depends on harvested energy procured from the RF signals. Also, all the relay nodes are provided with well-defined energy and information receivers [29] which can transition between EH and IF mode at the beginning of each transmission block. Moreover, each relay node has an EH circuit to convert the received RF power to direct current (DC) [5]. Without loss of generality, due to hefty deteriorations like deep fading and shadowing no direct-link between the user pairs is considered. In addition, all the channels are considered to be Rayleigh flat fading, i.e., the channel coefficients remain constant at one time block $\mathcal{T}$, and are perfectly known to all the relay nodes.

The transmission process takes place in two-phases, multiple access (MA) and broadcast (BC) phase. Firstly in MA phase, the K source nodes transmit their intended signals to the J EH relay nodes, all of which harvests energy from the procured RF signals employing EHTS protocol. The architecture of EHTS protocol based relay nodes is depicted in Fig. 2a. Later in the BC phase, the *selected* relay node(s) broadcast the amplified signal(s) to the K destination nodes. The communication block diagram for EH and IF at the j^{th} relay node employing EHTS protocol is presented by Fig. 2b. The EH receiver divides the total time block $\mathcal{T}$ into three chunks, firstly $\alpha_j^m \mathcal{T}$ for EH, secondly in two equal segments of $(1-\alpha_j^m)\mathcal{T}/2$ for information forwarding in MA and BC phase, with $0 \leq \alpha_j^m \leq 1, \ \forall j, m$, with $m \in \{1, \ldots, N_{sc}\}$. Note that α_j^m creates a balance between EH and IF modes for each relay node.

A. Energy-Harvesting (EH) Mode

In the MA phase, the K source nodes simultaneously transmit their intended RF signals to the J EH relay nodes, that is directed to their respective EH and IF receivers. The signal received by the j^{th} relay on m^{th} subcarrier, is given by

$$y_{\mathrm{E}_{\mathrm{R}_j}}^m = \sum_{k=1}^{K} h_{\mathrm{S}_k\mathrm{R}_j}^m \sqrt{P_{\mathrm{S}_k}^m} x_{\mathrm{S}_k}^m + n_{\mathrm{R}_j}^m, \tag{1}$$

where $h_{\mathrm{S}_k\mathrm{R}_j}^m$ and $x_{\mathrm{S}_k}^m$ denote the first-hop channel gain and the signal transmitted by the k^{th} source node to j^{th} relay node, with $\mathbb{E}|x_{\mathrm{S}_k}^m|^2 = 1$. Also, $n_{\mathrm{R}_j}^m$ and $P_{\mathrm{S}_k}^m$ represent the additive white gaussian noise (AWGN) at the j^{th} relay node, with $\mathbb{E}|n_{\mathrm{R}_j}^m|^2 = \sigma_{\mathrm{R}_j}^{m^2}$ and k^{th} source node' transmission power. Using (1), the harvested energy at j^{th} relay node is denoted as

$$\mathbb{E}_{\mathrm{h}_j}^m = \eta \alpha_j^m \mathcal{T} \sum_{k=1}^{K} P_{\mathrm{S}_k}^m \left| h_{\mathrm{S}_k\mathrm{R}_j}^m \right|^2 \tag{2}$$

where $0 \leq \eta \leq 1$ indicates the energy conversion efficiency, that remains directly proportional to the employed EH circuitry and rectification procedure [5]. For the sake of simplicity, we normalise the block to unit hereafter, i.e., $\mathcal{T} = 1$.

[1]We use "user-pairs" (U_{P_k}) and "source and destination pairs" $(S_k - D_k)$ interchangeably in this paper.

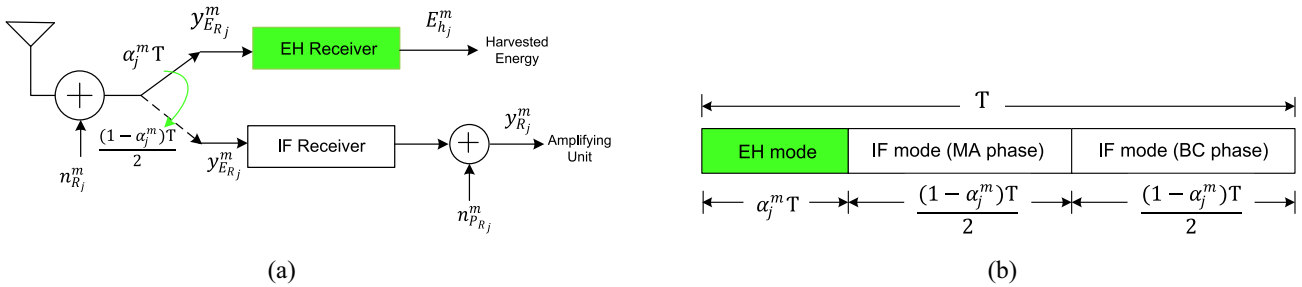

(a) (b)

Fig. 2. Illustration for EHTS protocol. (a) Architecture diagram of EHTS protocol. (b) Time block diagram of EHTS protocol.

B. Information-Forwarding (IF) Mode

The signal received at the information forwarding (IF) receivers can be written as

$$y^m_{\mathrm{R}_j} = y^m_{\mathrm{E}_{\mathrm{R}_j}} + n^m_{\mathrm{P}_{\mathrm{R}_j}}, \tag{3}$$

where $n^m_{\mathrm{P}_{\mathrm{R}_j}}$ represents the additional AWGN down-conversion processing and antenna noise with zero mean, and variance $\sigma^{m^2}_{\mathrm{P}_{\mathrm{R}_j}}$. In the BC phase, the *selected* relay node(s) amplifies the input signals and broadcast it to the destination nodes. Further, the normalised amplification factor on the $(m,n)^{\mathrm{th}}$ subcarrier pair, for $n \in \{1,\ldots,N_{sc}\}$, is written as

$$\kappa^{m,n}_{j,k} = \sqrt{P^n_{\mathrm{R}_j} \Big/ \sum\nolimits_{k=1}^{K} P^m_{\mathrm{S}_k} \left|h^m_{\mathrm{S}_k\mathrm{R}_j}\right|^2 + \sigma^{m^2}_{\mathrm{R}_j} + \sigma^{m^2}_{\mathrm{P}_{\mathrm{R}_j}}} \tag{4}$$

where $P^n_{\mathrm{R}_j}$ is the j^{th} relay's transmission power on n^{th} subcarrier. Thereby, the signal received at the k^{th} destination node can be given by using (3) and (4) as follows

$$y^{m,n}_{\mathrm{R}_j\mathrm{D}_k} = h^n_{\mathrm{R}_j\mathrm{D}_k}\kappa^{m,n}_{j,k}\Bigg(\underbrace{h^m_{\mathrm{S}_k\mathrm{R}_j}\sqrt{P^m_{\mathrm{S}_k}}x^m_{\mathrm{S}_k}}_{\text{Desired Signal}} + \underbrace{\sum\nolimits_{l=1,l\neq k}^{K} h^m_{\mathrm{S}_l\mathrm{R}_j}\sqrt{P^m_{\mathrm{S}_l}}x^m_{\mathrm{S}_l}}_{\text{Multi-user Interference}} + \underbrace{n^m_{\mathrm{R}_j} + n^m_{\mathrm{P}_{\mathrm{R}_j}}}_{\text{Relay Noise}}\Bigg) + n^n_{\mathrm{D}_k}, \tag{5}$$

where $h^n_{\mathrm{R}_j\mathrm{D}_k}$ and $n^n_{\mathrm{D}_k}$ represent the second-hop channel gain and AWGN for the j^{th} relay and k^{th} destination node on n^{th} subcarrier in BC phase, with $\mathbb{E}|n^n_{\mathrm{D}_k}|^2 = \sigma^{n^2}_{\mathrm{D}_k}$. Thus, the received signal-to-interference-and-noise-ratio (SINR) for the k^{th} destination node is given in (6), as shown at the top next page.

C. Relay Selection and Physical Layer Modelling

In general, the optimal relay selection criteria would be to select a set of relay nodes $\mathcal{C}$, so as to maximize the received SINR at the destination nodes, thereby increasing the average throughput, where $\mathcal{C} = \sum_{j=1}^{J} \mathcal{M}_j$, with $\mathcal{M}_j, \forall j$ being a binary indicator, such that $\mathcal{M}_j = 1$ if the j^{th} relay is selected and $\mathcal{M}_j = 0$ otherwise. But determining the best possible relay set is exponentially difficult in a multi-user multi-carrier scenario. In particular, each relay can choose to assist user pairs or not. Further, each relay can be paired with any number of user pairs U_P, therefore leading to $(K2^J - 1)$ possible combinations denoted by set $\mathcal{S}$, herein we exclude the scenario where no relay is selected. Moreover, each subcarrier in the MA phase can be paired with each subcarrier in BC phase in $N_{sc}!$ possible ways and each paired subcarrier can be allocated to the relay and user pairs in $(KJ)^{N_{sc}}$ possible combinations. This makes the problem NP hard to solve [26]. Therefore, there is a need for a less complex solution instead of exhaustive search (ES). Firstly, using (5) and (6) we define the subcarrier permutation matrix $\mathbf{\Phi} = \{\Phi^{m,n},\ \forall m,n\}$, where $\Phi^{m,n} \in \{0,1\}$ denotes the subcarrier pairing index. It is set as $\Phi^{m,n} = 1$, when m^{th} subcarrier in MA phase is paired with n^{th} subcarrier in BC phase and $\Phi^{m,n} = 0$, otherwise. Thus the subcarrier pairing conditions can be modelled as

$$(C.1) \quad \sum\nolimits_{m=1}^{N_{sc}} \Phi^{m,n} = 1,\ \forall\, n, \tag{7}$$

$$(C.2) \quad \sum\nolimits_{n=1}^{N_{sc}} \Phi^{m,n} = 1,\ \forall\, m, \tag{8}$$

Secondly, for the $(m,n)^{\mathrm{th}}$ paired subcarrier we employ a subcarrier pair based user allocation $\mathbf{\Lambda} = \{\Lambda^{m,n}_k,\ \forall k,m,n\}$ policy, by the aid of $\Lambda^{m,n}_k$ binary decision variable, with $\Lambda^{m,n}_k = 1$ if $(m,n)^{\mathrm{th}}$ subcarrier pair is allocated to the k^{th} user pair, whereas $\Lambda^{m,n}_k = 0$ elsewhere, given by

$$(C.3) \quad \sum\nolimits_{k=1}^{K} \Lambda^{m,n}_k = 1,\ \forall\, m,n \tag{9}$$

Thirdly, for determining the optimal relay set $\mathcal{C}$ it becomes imperative to address the following questions (1) how many relays should cooperate? (2) what user pairs to allocate the selected relay(s)? (3) what will be the subcarrier allocation for selected relay(s)? and most importantly (4) should a relay node be selected based on the available harvested energy? We address all of these questions by proposing a *relay selection strategy* that selects the relay set $\mathcal{C}$ from $\mathcal{S}$ based on the (*i*) subcarrier pairing and (*ii*) available energy at each relay node as shown below

1) For $(m,n)^{\mathrm{th}}$ paired subcarrier we employ a subcarrier based relay selection policy, $\mathbf{\Omega} = \{\Omega^{m,n}_j,\ \forall j,m,n\}$, with the help of $\Omega^{m,n}_j$ binary decision variable, wherein $\Omega^{m,n}_j = 1$ if $(m,n)^{\mathrm{th}}$ subcarrier pair is allocated to the j^{th} relay, whereas $\Omega^{m,n}_j = 0$ elsewhere, given by

$$(C.4) \quad \sum\nolimits_{j=1}^{J} \Omega^{m,n}_j = 1,\ \forall\, m,n \tag{10}$$

$$\Upsilon_{k,j}^{m,n} = \frac{P_{\mathrm{R}_j}^{n} P_{\mathrm{S}_k}^{m} \left| h_{\mathrm{S}_k\mathrm{R}_j}^{m} h_{\mathrm{R}_j\mathrm{D}_k}^{n} \right|^2}{\left| h_{\mathrm{R}_j\mathrm{D}_k}^{n} \right|^2 P_{\mathrm{R}_j}^{n} \left(\sum_{l\neq k}^{K} P_{\mathrm{S}_l}^{m} \left| h_{\mathrm{S}_l\mathrm{R}_j}^{m} \right|^2 + \sigma_{\mathrm{R}_j}^{m^2} + \sigma_{\mathrm{P}_{\mathrm{R}_j}}^{m^2} \right) + \sigma_{\mathrm{D}_k}^{n^2} \left(\sum_{k=1}^{K} P_{\mathrm{S}_k}^{m} \left| h_{\mathrm{S}_k\mathrm{R}_j}^{m} \right|^2 + \sigma_{\mathrm{R}_j}^{m^2} + \sigma_{\mathrm{P}_{\mathrm{R}_j}}^{m^2} \right)} \tag{6}$$

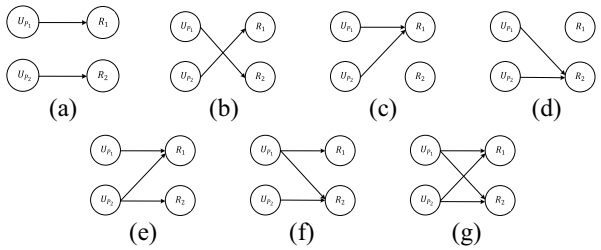

Fig. 3. Possible relay and user-pair pairing for $K = 2$ and $J = 2$. (a) Model 1. (b) Model 2. (c) Model 3. (d) Model 4. (e) Model 5. (f) Model 6. (g) Model 7.

To get better insight on the feasibility of subcarrier allocation based relay selection strategy, now we analyse all the possible cases for the paired subcarrier pair in two transmission hops.

- C_1. $\mathbf{N_{sc} < K, J}$: Let $K = J = 2$ and $N_{sc} = 1$. From (*C*.3) each paired subcarrier can be assigned to only one user, thus only a single user pairs is served. Therefore, in order to *server all the user pairs we must have* $N_{sc} \geq K$ *always*.
- C_2. $\mathbf{N_{sc} = K = J}$: Let $K = J = N_{sc} = 2$. Then only model $1-4$ are possible because of the constraints (*C*.1)$-$(*C*.4), i.e., each paired subcarrier is allocated to only a single user and relay. Thus, *if* $N_{sc} \leq J$ *then at most* N_{sc} *number of relays can be selected*.
- C_3. $\mathbf{N_{sc} = K < J}$: Let $N_{sc} = K = 2$ and $J = 3$. Since the number of possible combinations is very large, we don't elaborate here for brevity, but it can be directly considered similar to C_2 and we can say that *at most* N_{sc} *number of relay nodes can be selected*.
- C_4. $\mathbf{N_{sc} = K > J}$: Let $N_{sc} = K = 4$ and $J = 3$. Directly from the constraints (*C*.1)$-$(*C*.4), we can say that *always atleast* $(K - J + 1)$ *user pairs share the same relay nodes*.
- C_5. $\mathbf{N_{sc} = J < K}$: This case should be avoided in practice, directly implying from C_1.
- C_6. $\mathbf{N_{sc} = J > K}$: Let $N_{sc} = J = 3$ and $K = 2$. Directly, *all the users are served and always atleast* $(K - N_{sc})$ *user pairs gets additional* $(K - N_{sc})$ *subcarriers*.
- C_7. $\mathbf{N_{sc} > K, J}$: Let $K = J = 2$ and $N_{sc} = 4$. Then all the models $1-7$ are possible satisfying the constraints (*C*.1)$-$(*C*.4). Thus, *all the users are served and always at least* $(N_{sc} - K)$ *user pairs get additional* $(N_{sc} - K)$ *subcarriers*.

2) In view of the random nature of RF EH, we bound the total power utilized by each relay node, i.e., relay transmission power and its static power dissipation P_Q (by circuitry components), by the total harvested energy. It is important to note that static power dissipation is only considered when the j^{th} relay is selected. The *energy causality constraint* is given by

$$(C.5) \quad \sum_{m=1}^{N_{sc}} \sum_{n=1}^{N_{sc}} \Omega_j^{m,n} \Phi^{m,n} \frac{\left(1 - \alpha_j^m\right)\mathcal{T}}{2} P_{\mathrm{R}_j}^{n} + \mathcal{M}_j P_Q \leq \sum_{m=1}^{N_{sc}} \mathbb{E}_{\mathrm{h}_j}^{m}, \ \forall j. \tag{11}$$

Remark 1: It is really important to include relay static power dissipation P_Q in energy causality constraint for two reasons, firstly, a j^{th} relay node is only selected if its harvested energy is at least greater than its static power dissipation, secondly, it helps in determining the actual power available for transmission in second-hop, for each j^{th} relay node.

D. Energy-Efficiency (EE) Analysis

Using (6)-(11), the maximum achievable throughput can be given by

$$\mathcal{R}_T(\boldsymbol{\alpha}, \boldsymbol{P}_{\mathrm{S}}, \boldsymbol{P}_{\mathrm{R}}, \boldsymbol{\Phi}, \boldsymbol{\Omega}, \boldsymbol{\Lambda}) = \sum_{k=1}^{K} \sum_{j=1}^{J} \sum_{m=1}^{N_{sc}} \sum_{n=1}^{N_{sc}} \frac{\left(1 - \alpha_j^m\right)}{2} \Phi^{m,n} \Lambda_k^{m,n} \Omega_j^{m,n} \times \log_2\left(1 + \Upsilon_{k,j}^{m,n}\right), \tag{12}$$

where 1/2 occurs due to two-phase transmission and $\boldsymbol{\alpha} = \{\alpha_j^m\}$. The total power consumption in the network can be given by

$$\mathcal{P}_T(\boldsymbol{P}_{\mathrm{S}}, \boldsymbol{P}_{\mathrm{R}}, \boldsymbol{\Phi}, \boldsymbol{\Omega}, \boldsymbol{\Lambda}) = \sum_{k=1}^{K} \sum_{j=1}^{J} \sum_{m=1}^{N_{sc}} \sum_{n=1}^{N_{sc}} \Phi^{m,n} \Lambda_k^{m,n} \Omega_j^{m,n} \left(P_{\mathrm{S}_k}^{m} + P_{\mathrm{R}_j}^{n}\right) + 2KP_C + \mathcal{C}P_Q \tag{13}$$

where similar to P_Q, P_C denotes the static power dissipation by disparate chip components like feeder etc, for the user nodes. Next, we define EE as follows:

Definition 1: We can define EE as the desirability of the network model in achieving maximum number of successful end-to-end data bits transmission via the aid of relay node(s) weighted by the inverse of total transmitting and processing powers dissipated, given by

$$\varepsilon(\boldsymbol{\alpha}, \boldsymbol{P}_{\mathrm{S}}, \boldsymbol{P}_{\mathrm{R}}, \boldsymbol{\Phi}, \boldsymbol{\Omega}, \boldsymbol{\Lambda}) = \frac{\mathcal{R}_T(\boldsymbol{\alpha}, \boldsymbol{P}_{\mathrm{S}}, \boldsymbol{P}_{\mathrm{R}}, \boldsymbol{\Phi}, \boldsymbol{\Omega}, \boldsymbol{\Lambda})}{\mathcal{P}_T(\boldsymbol{P}_{\mathrm{S}}, \boldsymbol{P}_{\mathrm{R}}, \boldsymbol{\Phi}, \boldsymbol{\Omega}, \boldsymbol{\Lambda})}. \tag{14}$$

III. Problem Formulation and Transformation

The main objective of this work is to maximize the network's EE by jointly optimizing the EHTS time-block, relay selection, subcarrier permutation and allocation and transmit power at the nodes. Further, the problem targets to remain bounded by the network's power and energy causality regulation while simultaneously satisfying the suppression of

channel interferences. Therefore, the primal EEM problem can be formulated as shown below

$$
\begin{aligned}
(\mathbf{OP1}) \quad \max_{\boldsymbol{\alpha},\boldsymbol{P}_{\mathrm{S}},\boldsymbol{P}_{\mathrm{R}},\boldsymbol{\Phi},\boldsymbol{\Omega},\boldsymbol{\Lambda}} \quad & \varepsilon(\boldsymbol{\alpha},\boldsymbol{P}_{\mathrm{S}},\boldsymbol{P}_{\mathrm{R}},\boldsymbol{\Phi},\boldsymbol{\Omega},\boldsymbol{\Lambda}) \\
\text{subject to} \quad & (C.1)-(C.5), \\
& (C.6)\ \textstyle\sum_{k=1}^{K}\sum_{m=1}^{N_{sc}} P_{\mathrm{S}_k}^{m} \le P_{\max}; \\
& (C.7)\ \Phi^{m,n}\in\{0,1\},\ \Lambda_k^{m,n}\in\{0,1\}, \\
& \Omega_j^{m,n}\in\{0,1\}, \quad \forall\, k,j,m,n; \\
& (C.8)\ P_{\mathrm{S}_k}^{m}\ge 0,\ P_{\mathrm{R}_j}^{n}\ge 0, \alpha_j^{m}\ge 0, \\
& \forall\, k,j,m,n
\end{aligned} \tag{15}
$$

where $P_{\max}$ is the source transmission power budget.[2] Further, constraint (C.1) and (C.2) ensure that each subcarrier in MA phase is paired with a subcarrier in the BC phase, (C.3) and (C.4) establish that each paired subcarrier is allocated to one-and-only-one user pair and relay node respectively, (C.5) mandates that the energy utilisation by relay nodes never exceed their harvested energy, and (C.6) bounds the network's transmit power regulation.

Remark 2: The primal EEM problem **(OP1)** is a joint problem of discrete (binary) variables $\{\Phi^{m,n},\Lambda_k^{m,n},\Omega_j^{m,n}\}$ and continuous variables $\{P_{\mathrm{S}_k}^{m},\ P_{\mathrm{R}_j}^{n},\alpha_j^{m}\}$, i.e., of the non-convex mixed integer non-linear programming problem (MINLP) form. Unequivocally there is no standard way to procure its optimal solution, except an *exhaustive search* (ES) over all the feasible combinations of relay, subcarrier and user allocation, whilst augmenting the EE for each subcarrier permutation. But ES is unrealistic due to its lofty complexity.

Accordingly, we transform the non-convex primal problem to its tractable form as follows

- T_1: Firstly, we relieve the discrete variables as $\{\hat{\Phi}^{m,n},\hat{\Lambda}_k^{m,n},\hat{\Omega}_j^{m,n}\}\in[0,1]$, i.e., each subcarrier pair can be allocated to multiple relays and users, contrary to exclusive allocation. However, power allocated to each subcarrier pair regulates the multi-relay and multi-user interferences.
- T_2: Secondly, we apply change of variables, such that $\hat{P}_{\mathrm{S}_k}^{m}=\ln P_{\mathrm{S}_k}^{m}$ and $\hat{P}_{\mathrm{R}_j}^{n}=\ln P_{\mathrm{R}_j}^{n}$.
- T_3: Thirdly, we remodel the energy causality constraint (C.5) to a tractable form, (C.5a) and (C.5b), by including an auxiliary variable $\Sigma_j,\ \forall j$.
- T_4: Fourthly, we apply SCA method, to impose a lower bound on the throughput with coefficients $\{\boldsymbol{\gamma},\boldsymbol{\delta}\}=\{\gamma_{k,j}^{m,n},\delta_{k,j}^{m,n}\}$ and remodel the objective function into a concave-over-convex form. These coefficients are defined as $\gamma_{k,j}^{m,n}=\xi_{k,j}^{m,n}/(1+\xi_{k,j}^{m,n})$ and $\delta_{k,j}^{m,n}=\log_2(1+\xi_{k,j}^{m,n})-\gamma_{k,j}^{m,n}\log_2(\xi_{k,j}^{m,n})$ for any $\xi_{k,j}^{m,n}(t)>0$. The lower bound satisfies the equality to objective function when $\gamma_{k,j}^{m,n}=\hat{\Upsilon}_{k,j}^{m,n}/(1+\hat{\Upsilon}_{k,j}^{m,n})$ and $\delta_{k,j}^{m,n}=\log_2(1+\hat{\Upsilon}_{k,j}^{m,n})-\gamma_{k,j}^{m,n}\times\log_2(\hat{\Upsilon}_{k,j}^{m,n})$ and the equality holds *iff* $(\gamma_{k,j}^{m,n},\delta_{k,j}^{m,n})=(1,0)$ and $\hat{\Upsilon}_{k,j}^{m,n}\to\infty$.
- T_5: Lastly, we apply the Dinkelbach's method [27] to the fractional concave-over-convex objective function, thereby converting it to a subtractive form, by the introduction of a positive penalty factor Ψ paid for resource utilization.[3]

Now, the transformed primal problem for fixed EHTS time block and penalty factor is given by

$$
\begin{aligned}
(\mathbf{OP2a}) \quad \max_{\hat{\boldsymbol{P}}_{\mathrm{S}},\hat{\boldsymbol{P}}_{\mathrm{R}},\boldsymbol{\Sigma},\hat{\boldsymbol{\Phi}},\hat{\boldsymbol{\Omega}},\hat{\boldsymbol{\Lambda}}} \quad & \hat{\varepsilon}\Big(\boldsymbol{\alpha},\hat{\boldsymbol{P}}_{\mathrm{S}},\hat{\boldsymbol{P}}_{\mathrm{R}},\hat{\boldsymbol{\Phi}},\hat{\boldsymbol{\Omega}},\hat{\boldsymbol{\Lambda}}\Big) \\
\text{subject to} \quad & (C.1)\ \textstyle\sum_{m=1}^{N_{sc}}\hat{\Phi}^{m,n}=1, \qquad \forall\, n; \\
& (C.2)\ \textstyle\sum_{n=1}^{N_{sc}}\hat{\Phi}^{m,n}=1, \qquad \forall\, m; \\
& (C.3)\ \textstyle\sum_{k=1}^{K}\hat{\Lambda}_k^{m,n}=1, \qquad \forall\, m,n; \\
& (C.4)\ \textstyle\sum_{j=1}^{J}\hat{\Omega}_j^{m,n}=1, \qquad \forall\, m,n; \\
& (C.5a)\ \textstyle\sum_{m=1}^{N_{sc}}\sum_{n=1}^{N_{sc}}\hat{\Omega}_j^{m,n}\hat{\Phi}^{m,n}\frac{(1-\alpha_j^{m})\mathcal{T}}{2} \\
& \quad\times e^{\hat{P}_{\mathrm{R}_j}^{n}}+\mathcal{M}_j P_Q-\Sigma_j\le 0, \quad \forall\, j; \\
& (C.5b)\ \textstyle\sum_{m=1}^{N_{sc}}\hat{\mathbb{E}}_{\mathrm{h}_j}^{m}\le\Sigma_j, \qquad \forall\, j; \\
& (C.6)\ \textstyle\sum_{k=1}^{K}\sum_{m=1}^{N_{sc}} e^{\hat{P}_{\mathrm{S}_k}^{m}}\le P_{\max}, \\
& (C.7)\ \hat{\Phi}^{m,n}\in[0,1],\ \hat{\Lambda}_k^{m,n}\in[0,1],\ \hat{\Omega}_j^{m,n}\in[0,1], \\
& \qquad\qquad \forall\, k,j,m,n; \\
& (C.8)\ e^{\hat{P}_{\mathrm{S}_k}^{m}}\ge 0,\ e^{\hat{P}_{\mathrm{R}_j}^{n}}\ge 0, \quad \forall\, k,j,m,n
\end{aligned} \tag{16}
$$

where $\hat{\varepsilon}(\boldsymbol{\alpha},\hat{\boldsymbol{P}}_{\mathrm{S}},\hat{\boldsymbol{P}}_{\mathrm{R}},\hat{\boldsymbol{\Phi}},\hat{\boldsymbol{\Omega}},\hat{\boldsymbol{\Lambda}})=\hat{\mathcal{R}}_T(\boldsymbol{\alpha},\hat{\boldsymbol{P}}_{\mathrm{S}},\hat{\boldsymbol{P}}_{\mathrm{R}},\hat{\boldsymbol{\Phi}},\hat{\boldsymbol{\Omega}},\hat{\boldsymbol{\Lambda}})-\Psi\hat{\mathcal{P}}_T(\hat{\boldsymbol{P}}_{\mathrm{S}},\hat{\boldsymbol{P}}_{\mathrm{R}},\hat{\boldsymbol{\Phi}},\hat{\boldsymbol{\Omega}},\hat{\boldsymbol{\Lambda}})$ and $\hat{\mathcal{R}}_T(\boldsymbol{\alpha},\hat{\boldsymbol{P}}_{\mathrm{S}},\hat{\boldsymbol{P}}_{\mathrm{R}},\hat{\boldsymbol{\Phi}},\hat{\boldsymbol{\Omega}},\hat{\boldsymbol{\Lambda}})$ and $\hat{\mathcal{P}}_T(\hat{\boldsymbol{P}}_{\mathrm{S}},\hat{\boldsymbol{P}}_{\mathrm{R}},\hat{\boldsymbol{\Phi}},\hat{\boldsymbol{\Omega}},\hat{\boldsymbol{\Lambda}})$ are defined in (17) and (18), as shown on the top of the next page. Further

$$
\hat{\mathbb{E}}_{\mathrm{h}_j}^{m}=\eta\alpha_j^{m}\mathcal{T}\sum_{k=1}^{K} e^{\hat{P}_{\mathrm{S}_k}^{m}}\left|h_{\mathrm{S}_k\mathrm{R}_j}^{m}\right|^2; \tag{19}
$$

and $\hat{\Upsilon}_{k,j}^{m,n}$ is given in (20), as shown at the top of the next page.

For the optimally obtained resource allocation policy, we obtain the EHTS time block $\boldsymbol{\alpha}$, by applying change of variable, $\hat{\alpha}_j^{m}=\left(1-\alpha_j^{m}\right)$, as follows

$$
\begin{aligned}
(\mathbf{OP2b}) \quad \max_{\hat{\boldsymbol{\alpha}}} \quad & \dot{\varepsilon}\Big(\hat{\boldsymbol{\alpha}},\hat{\boldsymbol{P}}_{\mathrm{S}},\hat{\boldsymbol{P}}_{\mathrm{R}},\hat{\boldsymbol{\Phi}},\hat{\boldsymbol{\Omega}},\hat{\boldsymbol{\Lambda}}\Big) \\
\text{subject to} \quad & (C.5)\ \textstyle\sum_{m=1}^{N_{sc}}\sum_{n=1}^{N_{sc}}\hat{\Omega}_j^{m,n}\hat{\Phi}^{m,n}\frac{\hat{\alpha}_j^{m}}{2}P_{\mathrm{R}_j}^{n} \\
& \quad+\mathcal{M}_j P_Q\le\textstyle\sum_{m=1}^{N_{sc}}\mathbb{E}_{\mathrm{h}_j}^{m}, \quad \forall\, j; \\
& (C.8)\ \alpha_j^{m}\ge 0,
\end{aligned} \tag{21}
$$

where $\dot{\varepsilon}_{LB}=\dot{\mathcal{R}}_T/\hat{\mathcal{P}}_T$, $\dot{\mathbb{E}}_{\mathrm{h}_j}^{m}=\eta(1-\hat{\alpha}_j^{m})\mathcal{T}\sum\limits_{k=1}^{K} e^{\hat{P}_{\mathrm{S}_k}^{m}}|h_{\mathrm{S}_k\mathrm{R}_j}^{m}|^2$ and

$$
\begin{aligned}
\dot{\mathcal{R}}_T=&\sum_{k=1}^{K}\sum_{j=1}^{J}\sum_{m=1}^{N_{sc}}\sum_{n=1}^{N_{sc}}\frac{\hat{\alpha}_j^{m}}{2}\hat{\Phi}^{m,n}\hat{\Lambda}_k^{m,n}\hat{\Omega}_j^{m,n} \\
&\times\left(\frac{\gamma_{k,j}^{m,n}}{\ln(2)}\ln\left(\hat{\Upsilon}_{k,j}^{m,n}\right)+\delta_{k,j}^{m,n}\right)
\end{aligned} \tag{22}
$$

[2]In this work, the relay nodes procure energy solely from the source's RF signals, thus the network's transmit power budget is specifically confined for the source nodes only.

[3]When $\Psi\to 0$ this suggest that penalty paid for resource allocation is zero and the problem becomes a sum-rate maximisation problem, while when $\Psi\to\infty$, then no resource allocation policy will be good enough to maximize the EE of the network.

$$\hat{\mathcal{R}}_T\Big(\boldsymbol{\alpha}, \hat{\boldsymbol{P}}_{\mathrm{S}}, \hat{\boldsymbol{P}}_{\mathrm{R}}, \hat{\boldsymbol{\Phi}}, \hat{\boldsymbol{\Omega}}, \hat{\boldsymbol{\Lambda}}\Big) = \sum_{k=1}^{K}\sum_{j=1}^{J}\sum_{m=1}^{N_{sc}}\sum_{n=1}^{N_{sc}} \frac{\left(1-\alpha_j^m\right)}{2}\hat{\Phi}^{m,n}\hat{\Lambda}_k^{m,n}\hat{\Omega}_j^{m,n}\left(\frac{\gamma_{k,j}^{m,n}}{\ln(2)}\ln\Big(\hat{\Upsilon}_{k,j}^{m,n}\Big)+\delta_{k,j}^{m,n}\right) \quad (17)$$

$$\hat{\mathcal{P}}_T\Big(\hat{\boldsymbol{P}}_{\mathrm{S}}, \hat{\boldsymbol{P}}_{\mathrm{R}}, \hat{\boldsymbol{\Phi}}, \hat{\boldsymbol{\Omega}}, \hat{\boldsymbol{\Lambda}}\Big) = \sum_{k=1}^{K}\sum_{j=1}^{J}\sum_{m=1}^{N_{sc}}\sum_{n=1}^{N_{sc}} \hat{\Phi}^{m,n}\hat{\Lambda}_k^{m,n}\hat{\Omega}_j^{m,n}\left(e^{\hat{P}_{\mathrm{S}_k}^m}+e^{\hat{P}_{\mathrm{R}_j}^n}\right)+2KP_C+\mathcal{C}P_Q \quad (18)$$

$$\hat{\Upsilon}_{k,j}^{m,n} = \frac{e^{\hat{P}_{\mathrm{R}_j}^n+\hat{P}_{\mathrm{S}_k}^m}\left|h_{\mathrm{S}_k\mathrm{R}_j}^m h_{\mathrm{R}_j\mathrm{D}_k}^n\right|^2}{\left|h_{\mathrm{R}_j\mathrm{D}_k}^n\right|^2 e^{\hat{P}_{\mathrm{R}_j}^n}\left(\sum_{l\neq k}^{K} e^{\hat{P}_{\mathrm{S}_l}^m}\left|h_{\mathrm{S}_l\mathrm{R}_j}^m\right|^2+\sigma_{\mathrm{R}_j}^{m^2}+\sigma_{\mathrm{P}_{\mathrm{R}_j}}^{m^2}\right)+\sigma_{\mathrm{D}_k}^{n^2}\left(\sum_{k=1}^{K} e^{\hat{P}_{\mathrm{S}_k}^m}\left|h_{\mathrm{S}_k\mathrm{R}_j}^m\right|^2+\sigma_{\mathrm{R}_j}^{m^2}+\sigma_{\mathrm{P}_{\mathrm{R}_j}}^{m^2}\right)} \quad (20)$$

Theorem 1: For any given $\{\gamma_{k,j}^{m,n}, \delta_{k,j}^{m,n}, \Psi\}$ and fixed $(\hat{\Phi}^{m,n}\hat{\Lambda}_k^{m,n}\hat{\Omega}_j^{m,n})$, the lower bound in transformation T_4 is concavified by the transformation in T_2 for (**OP2a**) and additionally by $\hat{\alpha}_j^m = (1-\alpha_j^m)$ for (**OP2b**), the problems are quasi-concave in nature.

Proof: The proof is relegated to Appendix A. ■

IV. EEM Resource Allocation Algorithm

In this section, we describe the proposed iterative EEM algorithm and find the expressions for the optimal resource allocation variables. For fixed coefficients $\{\boldsymbol{\gamma}, \boldsymbol{\delta}\}$ and given $\{\hat{\boldsymbol{\Phi}}, \hat{\boldsymbol{\Omega}}, \hat{\boldsymbol{\Lambda}}\}$ and Ψ, the problem (**OP2a**)((**OP2b**)) is quasi-concave. If the relay selection, subcarrier allocation and pairing matrices $(\boldsymbol{\Lambda}, \boldsymbol{\Omega}, \boldsymbol{\Phi})$ are not given then the transformed EEM optimization problem (**OP2a**)(**OP2b**) remains NP-hard to solve. By employing extensively studied NP-hard problem - the polynomial reduction with the help of the subset sum (SS), we can prove the NP-hardness of the transformed problem (**OP2a**)(**OP2b**), defined as below

Definition 2 (Subset Sum (SS)): Let us indicate the set of N_{sc} subcarriers by $\mathcal{N}$, also $\mathcal{W} = \{w_1, w_2, ...\}$ denote a set of natural numbers, and *V* represents a positive integer with $V < \sum_{w_l\in\mathcal{W}} w_l$. Now, we need to find that if a subset $\mathcal{N} \in \mathcal{W}$ exists, satisfying $\sum\mathcal{N} = V$, respectively.

It is to be noted that the solution to the SS is objective in nature, i.e., YES when the SS instance is satisfied and NO when the SS instance is not satisfied, respectively.

Decision version[4] of transformed EEM optimization problem (**OP2a**)(**OP2b**) - Suppose we have a set of subcarrier combinations denoted by *a* and non-decreasing rate-power functions given by *b* such that $a > b$. Then we need to determine that if there exist a set of user, subcarrier and relay permutations with total transmit power budget, such that energy causality constraint of the selected relay node is satisfied while meeting each user's request, moreover no same subcarrier is allocated to different relay node or user pair, respectively.

[4]Please note that hardness with respect to the computational complexity of the decision version and optimization problem remains identical, even though the answers to both of them are different, we elaborate the decision version, respectively.

Proposition 1: The transformed EEM optimization problem **(OP1)** formulated remains NP-hard to solve.

Proof: The proof is relegated to Appendix B. ■

It is evident from the literature, that as the total number of subcarriers approaches to infinity the duality gap between the dual and the optimization problem plummets to zero [30]. Therefore, after the transformation of the primal problem (**OP1**) to the problems (**OP2a**) and (**OP2b**), we aim to solve the transformed problems by solving their dual problems, respectively. Hence, we provide the following definition and theorems to elaborate on the same.

Definition 3 (Duality Gap): The difference between the optimal solutions procured through the transformed optimization problem (**OP2a**) and its dual problem (elaborated as (**DP1**) later in the paper), is referred as the duality gap.

Proposition 2: If we have a large number of subcarriers available N_{sc}, then the duality gap between the problem (**OP2a**) and its dual problem (**DP1**) will tend to zero.

Proof: The proof is presented in Appendix C. ■

Therefore, in this work we solve the dual problems of the transformed optimization problem and procure the optimal solutions jointly.

The Lagrangian function for the problem (**OP2a**) is given in (23), as shown at the top of the next page, where $\lambda, \boldsymbol{\varphi} = \{\varphi_j\}, \boldsymbol{\chi} = \{\chi_j\}$ are the Lagrangian multipliers associated with the constraints (*C*.6), (*C*.5*a*) and (*C*.5*b*) of optimization problem (**OP2a**).

Next, the dual problem can be readily expressed as

$$(\mathbf{DP1}) \min_{\lambda,\boldsymbol{\varphi},\boldsymbol{\chi}\geq 0} \max_{\substack{\hat{\boldsymbol{P}}_{\mathrm{S}},\hat{\boldsymbol{P}}_{\mathrm{R}}\\ \hat{\boldsymbol{\Phi}},\hat{\boldsymbol{\Omega}},\hat{\boldsymbol{\Lambda}},\boldsymbol{\Sigma}}} \mathcal{L}\Big(\hat{\boldsymbol{P}}_{\mathrm{S}}, \hat{\boldsymbol{P}}_{\mathrm{R}}, \hat{\boldsymbol{\Phi}}, \hat{\boldsymbol{\Omega}}, \hat{\boldsymbol{\Lambda}}, \boldsymbol{\Sigma}, \boldsymbol{\gamma}, \boldsymbol{\delta}, \lambda, \boldsymbol{\varphi}, \boldsymbol{\chi}\Big)$$
$$\text{subject to } (C.1)-(C.4), (C.7) \,\&\, (C.8). \quad (24)$$

The dual problem **(DP1)** is disintegrated into a master-slave problem and solved via two iterative steps: (*i*) first step is related to a subproblem for finding the solutions of the resource allocation, and (*ii*) second step involves a master dual problem for updating the Lagrangian multipliers.

We obtain the subproblem solution by exploiting Karush-Kuhn-Tucker (KKT) conditions. Firstly we get the optimal power allocation policy $(\hat{\boldsymbol{P}}_{\mathrm{S}}, \hat{\boldsymbol{P}}_{\mathrm{R}})$ at the $(u+1)$-th iteration by taking the partial derivative of (23) *w.r.t.* $\hat{P}_{S_k}^m$ and $\hat{P}_{R_j}^n$ and equating it to zero, yielding (25) and (26), as shown at the top

$$\mathcal{L}\Big(\hat{\boldsymbol{P}}_{\rm S},\hat{\boldsymbol{P}}_{\rm R},\hat{\boldsymbol{\Phi}},\hat{\boldsymbol{\Omega}},\hat{\boldsymbol{\Lambda}},\boldsymbol{\Sigma},\boldsymbol{\gamma},\boldsymbol{\delta},\lambda,\boldsymbol{\varphi},\boldsymbol{\chi}\Big)=\hat{\varepsilon}\Big(\boldsymbol{\alpha},\hat{\boldsymbol{P}}_{\rm S},\hat{\boldsymbol{P}}_{\rm R},\hat{\boldsymbol{\Phi}},\hat{\boldsymbol{\Omega}},\hat{\boldsymbol{\Lambda}},\boldsymbol{\gamma},\boldsymbol{\delta}\Big)-\lambda\Bigg(\sum\nolimits_{k=1}^{K}\sum\nolimits_{m=1}^{N_{sc}}e^{\hat{P}_{{\rm S}_k}^{m}}-P_{\max}\Bigg)$$
$$-\sum\nolimits_{j=1}^{J}\varphi_j\Bigg(\sum\nolimits_{m=1}^{N_{sc}}\sum\nolimits_{n=1}^{N_{sc}}\hat{\Omega}_j^{m,n}\hat{\Phi}^{m,n}\frac{\left(1-\alpha_j^m\right)}{2}e^{\hat{P}_{{\rm R}_j}^{n}}+\mathcal{M}_jP_Q-\Sigma_j\Bigg)-\sum\nolimits_{j=1}^{J}\chi_j\Bigg(\sum\nolimits_{m=1}^{N_{sc}}\hat{\mathbb{E}}_{{\rm h}_j}^{m}-\Sigma_j\Bigg) \quad (23)$$

$$e^{\hat{P}_{{\rm S}_k}^{m^2}}\Bigg(\Psi\sum\nolimits_{j=1}^{J}\sum\nolimits_{n=1}^{N_{sc}}\hat{\Phi}^{m,n}\hat{\Lambda}_k^{m,n}\hat{\Omega}_j^{m,n}+\lambda_t+\sum\nolimits_{j=1}^{J}\chi_j\eta\alpha_j^m\Big|h_{{\rm S}_k{\rm R}_j}^{m}\Big|^2\Bigg)\frac{\Big|h_{{\rm S}_k{\rm R}_j}^{m}\Big|^2}{\sigma_{R_j}^{(m)^2}+\sigma_{P_{{\rm R}_j}}^{(m)^2}}$$
$$+\;e^{\hat{P}_{{\rm S}_k}^{m}}\Bigg(\Psi\sum\nolimits_{j=1}^{J}\sum\nolimits_{n=1}^{N_{sc}}\hat{\Phi}^{m,n}\hat{\Lambda}_k^{m,n}\hat{\Omega}_j^{m,n}+\lambda_t+\sum\nolimits_{j=1}^{J}\chi_j\eta\alpha_j^m\Big|h_{{\rm S}_k{\rm R}_j}^{m}\Big|^2\Bigg)\Big(\Gamma_{{\rm R}_j{\rm D}_k}^{n}+1\Big)\Bigg(\sum\nolimits_{l\neq k}^{K}\Gamma_{{\rm S}_l{\rm R}_j}^{n}+1\Bigg)$$
$$-\sum\nolimits_{j=1}^{J}\sum\nolimits_{n=1}^{N_{sc}}\frac{\gamma_{k,j}^{m,n}(1-\alpha_j^m)}{2\ln(2)}\hat{\Phi}^{m,n}\hat{\Lambda}_k^{m,n}\hat{\Omega}_j^{m,n}\Big(\Gamma_{{\rm R}_j{\rm D}_k}^{n}+1\Big)\Bigg(\sum\nolimits_{l\neq k}^{K}\Gamma_{{\rm S}_l{\rm R}_j}^{n}+1\Bigg)=0 \quad (25)$$

$$e^{\hat{P}_{{\rm R}_j}^{n^2}}\Bigg(\Psi\sum\nolimits_{k=1}^{K}\sum\nolimits_{m=1}^{N_{sc}}\hat{\Phi}^{m,n}\hat{\Lambda}_k^{m,n}\hat{\Omega}_j^{m,n}+\varphi_j\sum\nolimits_{m=1}^{N_{sc}}\Omega_j^{m,n}\Phi^{m,n}\frac{\left(1-\alpha_j^m\right)}{2}\Bigg)\frac{\Big|h_{{\rm R}_j{\rm D}_k}^{n}\Big|^2}{\sigma_{D_k}^{(n)^2}}$$
$$+\;e^{\hat{P}_{{\rm R}_j}^{n}}\Bigg(\Psi\sum\nolimits_{k=1}^{K}\sum\nolimits_{m=1}^{N_{sc}}\hat{\Phi}^{m,n}\hat{\Lambda}_k^{m,n}\hat{\Omega}_j^{m,n}+\varphi_j\sum\nolimits_{m=1}^{N_{sc}}\Omega_j^{m,n}\Phi^{m,n}\frac{\left(1-\alpha_j^m\right)}{2}\Bigg)\Bigg(1+\frac{\Gamma_{{\rm S}_k{\rm R}_j}^{m}}{\sum_{l\neq k}\Gamma_{{\rm S}_l{\rm R}_j}^{m}+1}\Bigg)$$
$$-\sum\nolimits_{k=1}^{K}\sum\nolimits_{m=1}^{N_{sc}}\frac{\gamma_{k,j}^{m,n}\left(1-\alpha_j^m\right)}{2\ln(2)}\hat{\Phi}^{m,n}\hat{\Lambda}_k^{m,n}\hat{\Omega}_j^{m,n}\Bigg(1+\frac{\Gamma_{{\rm S}_k{\rm R}_j}^{m}}{\sum_{l\neq k}\Gamma_{{\rm S}_l{\rm R}_j}^{m}+1}\Bigg)=0 \quad (26)$$

of this page, respectively, where $\Gamma_{{\rm R}_j{\rm D}_k}^{n}=e^{\hat{P}_{{\rm R}_j}^{n}}\mid h_{{\rm R}_j{\rm D}_k}^{n}\mid^2/\sigma_{D_k}^{n^2}$, $\Gamma_{{\rm S}_l{\rm R}_j}^{m}=e^{\hat{P}_{S_l}^{m}}\mid h_{{\rm S}_l{\rm R}_j}^{m}\mid^2/(\sigma_{R_j}^{m^2}+\sigma_{P_{{\rm R}_j}}^{m^2})$. The solution to the quadratic equation $ax^2+bx-c=0$ can be given by $x=(-b\pm\sqrt{b^2+4ac})/2a$. By applying a linear approximation method [31], i.e., $\sqrt{a+b}\approx\sqrt{a}+\frac{b}{2\sqrt{a}}$, we get two possible solutions of *x* as *c*/*b* or $-$(*c*/*b* + *b*/*a*). As $x\geq 0$, we use *c*/*b* to update the solutions as in (27) and (28), as shown at the top of the next page.

Remark 3: It is evident from (27) and (28) that the optimal power allocation not only depends on the Lagrangian multipliers, but also on the network penalty Ψ and EHTS time block α_j^m. Herein, the inverse of the sum of associated Lagrangian multipliers, penalty factor and EHTS time block can be weighed as the water-filling level, to capture the effect of total transmit power budget $P_{\max}$. Moreover, (27) exhibits that the source power allocation has the channel inversion characteristics. However, in the case of absence of subcarrier-relay allocation and pairing, the power allocation likewise depends on the interference constituted by various users and relays.

Theorem 2: The optimal power allocation policy $(\hat{\boldsymbol{P}}_{\rm S}^{\star},\hat{\boldsymbol{P}}_{\rm R}^{\star})$ must satisfy $\Sigma_j^{\star}=\sum_{q=1}^{t}\sum_{m=1}^{N_{sc}}\hat{\mathbb{E}}_{{\rm h}_j}^{m},\forall j$.

Proof: We prove this theorem by contradiction. For $j^{\rm th}$ relay node, let us assume $\sum_{m=1}^{N_{sc}}\hat{\mathbb{E}}_{{\rm h}_j}^{m}<\Sigma_j$. This means that the upper limit set in (*C*.5*a*) for power dissipation at the $j^{\rm th}$ relay node, will be more than the harvested energy in the network. This directly violates the *energy causality constraint* (*C*.5), hence for optimal power allocation policy $\Sigma_j^{\star}=\sum_{m=1}^{N_{sc}}\hat{\mathbb{E}}_{{\rm h}_j}^{m},\forall j$. ■

For the obtained power allocation policy $(\hat{\boldsymbol{P}}_{\rm S}^{\star},\hat{\boldsymbol{P}}_{\rm R}^{\star},\boldsymbol{\Sigma}^{\star})$, the problem (**DP1**) is rewritten as

$$(\textbf{DP2})\;\max_{\hat{\boldsymbol{\Lambda}}}\;\sum\nolimits_{k=1}^{K}\sum\nolimits_{m=1}^{N_{sc}}\sum\nolimits_{n=1}^{N_{sc}}\hat{\Lambda}_k^{m,n}\Delta_k^{m,n}-\Theta$$
$$\text{subject to}\;\;(C.4)\;\&\;(C.7) \quad (29)$$

where $\Delta_k^{m,n}$ and Θ are defined in (30), as shown on the top of the next page. It is to be noted that $\Delta_k^{m,n}$ exclusively rely on subcarrier allocation, while Θ remains independent of any subcarrier-user combinations. Straightforwardly, for $(m,n)^{\rm th}$ subcarrier pair, the optimal subcarrier allocation to users is the one that maximizes $\Delta_{k,j}^{m,n}$ *w.r.t. k* as

$$\hat{\Lambda}_k^{m,n^{\star}}=\begin{cases}1, & \text{for } k=\arg\max_k\Delta_k^{m,n},\quad\forall\, m,n;\\ 0, & \text{otherwise}\end{cases} \quad (31)$$

Similarly, we can reformulate the problem for subcarrier pairing and relay selection as follows

$$(\textbf{DP3})\;\max_{\hat{\boldsymbol{\Phi}},\hat{\boldsymbol{\Omega}}}\;\sum\nolimits_{j=1}^{J}\sum\nolimits_{m=1}^{N_{sc}}\sum\nolimits_{n=1}^{N_{sc}}\hat{\Phi}^{m,n}\hat{\Omega}_j^{m,n}\Delta_j^{m,n}-(\Xi+\Theta)$$
$$\text{subject to}\;\;(C.1)-(C.3)\;\&\;(C.7) \quad (32)$$

where $\Theta=\Psi 2KP_c+\lambda(\sum_{k=1}^{K}\sum_{m=1}^{N_{sc}}e^{\hat{P}_{{\rm S}_k}^{m^{\star}}}-P_{\max})-\sum_{j=1}^{J}\varphi_j\Sigma_j^{\star}+\sum_{j=1}^{J}\chi_j(\sum_{m=1}^{N_{sc}}\hat{\mathbb{E}}_{{\rm h}_j}^{m^{\star}}-\Sigma_j^{\star})$, $\Delta_j^{m,n}$ is defined as in (33), as shown on the top of the next page, and

$$\Xi=P_Q\Bigg(\mathcal{C}\Psi+\sum\nolimits_{j=1}^{J}\varphi_j\mathcal{M}_j\Bigg). \quad (34)$$

Herein, $\Delta_j^{m,n}$ and Ξ depends on the subcarrier pairing and relay selection, whereas Θ remains independent of the same.

$$e^{\hat{P}^{m}_{\mathrm{S}_k}} = \left[\frac{\sum_{j=1}^{J}\sum_{n=1}^{N_{sc}}\gamma_{k,j}^{m,n}\left(1-\alpha_j^m\right)\hat{\Phi}^{m,n}\hat{\Lambda}_k^{m,n}\hat{\Omega}_j^{m,n}}{2\ln(2)\left(\Psi\sum_{j=1}^{J}\sum_{n=1}^{N_{sc}}\hat{\Phi}^{m,n}\hat{\Lambda}_k^{m,n}\hat{\Omega}_j^{m,n}+\lambda_t+\sum_{j=1}^{J}\chi_j\eta\alpha_j^m\left|h^m_{\mathrm{S}_k\mathrm{R}_j}\right|^2\right)}\right]^{+} \tag{27}$$

$$e^{\hat{P}^{n}_{\mathrm{R}_j}} = \left[\frac{\sum_{k=1}^{K}\sum_{m=1}^{N_{sc}}\gamma_{k,j}^{m,n}\left(1-\alpha_j^m\right)\hat{\Phi}^{m,n}\hat{\Lambda}_k^{m,n}\hat{\Omega}_j^{m,n}}{\ln(2)\left(2\Psi\sum_{k=1}^{K}\sum_{m=1}^{N_{sc}}\hat{\Phi}^{m,n}\hat{\Lambda}_k^{m,n}\hat{\Omega}_j^{m,n}+\sum_{m=1}^{N_{sc}}\hat{\Omega}_j^{m,n}\hat{\Phi}^{m,n}\left(1-\alpha_j^m\right)\varphi_j\right)}\right]^{+} \tag{28}$$

$$\Delta_k^{m,n} = \sum_{j=1}^{J}\hat{\Phi}^{m,n}\hat{\Omega}_j^{m,n}\left(\frac{\left(1-\alpha_j^m\right)}{2}\left(\frac{\gamma_{k,j}^{m,n}}{\ln(2)}\ln\left(\hat{\Upsilon}_{k,j}^{m,n^\star}\right)+\delta_{k,j}^{m,n}\right)-\Psi\left(e^{\hat{P}^{m^\star}_{\mathrm{S}_k}}+e^{\hat{P}^{n^\star}_{\mathrm{R}_j}}\right)\right)$$

$$\Theta = P_Q\left(\mathcal{C}\Psi+\sum\nolimits_{j=1}^{J}\varphi_j\mathcal{M}_j\right)+\Psi 2KP_c+\lambda\left(\sum\nolimits_{k=1}^{K}\sum\nolimits_{m=1}^{N_{sc}}e^{\hat{P}^{m^\star}_{\mathrm{S}_k}}-P_{\max}\right)$$
$$+\sum_{j=1}^{J}\varphi_j\left(\sum\nolimits_{m=1}^{N_{sc}}\sum\nolimits_{n=1}^{N_{sc}}\hat{\Omega}_j^{m,n}\hat{\Phi}^{m,n}\frac{\left(1-\alpha_j^m\right)}{2}e^{\hat{P}^{n^\star}_{\mathrm{R}_j}}+\mathcal{M}_jP_Q-\Sigma_j^{t^\star}\right)+\sum\nolimits_{j=1}^{J}\chi_j\left(\sum\nolimits_{m=1}^{N_{sc}}\hat{\mathbb{E}}^{m^\star}_{\mathrm{h}_j}-\Sigma_j^\star\right) \tag{30}$$

$$\Delta_j^{m,n} = \sum\nolimits_{k=1}^{K}\hat{\Lambda}_k^{m,n^\star}\left(\frac{\left(1-\alpha_j^m\right)}{2}\left(\frac{\gamma_{k,j}^{m,n}}{\ln(2)}\ln\left(\hat{\Upsilon}_{k,j}^{m,n^\star}\right)+\delta_{k,j}^{m,n}\right)-\Psi\left(e^{\hat{P}^{m^\star}_{\mathrm{S}_k}}+e^{\hat{P}^{n^\star}_{\mathrm{R}_j}}\right)\right)-\varphi_j\frac{\left(1-\alpha_j^m\right)}{2}e^{\hat{P}^{n^\star}_{\mathrm{R}_j}} \tag{33}$$

Thus, we obtain the optimal subcarrier allocation to relays as

$$\hat{\Omega}_j^{m,n^\star} = \begin{cases} 1, & \text{for } j = \arg\max_j \Delta_j^{m,n} - \Xi,\ \forall\ m,n; \\ 0, & \text{otherwise} \end{cases} \tag{35}$$

And on the similar grounds to the dual problem (**DP3**), for optimal $\hat{\Omega}_j^{m,n^\star}$, we can obtain the optimal subcarrier pairing policy as $\Phi^{m,n^\star} = \max_{k,j}\sum_{j=1}^{J}\hat{\Omega}_j^{m,n^\star}\Delta_j^{m,n} - \Xi,\ \forall m,n$ and can be solved very efficiently using any standard assignment algorithms like Hungarian algorithm [32].

Remark 4: The continuous sequence in **(DP2)** and **(DP3)** can be unconditionally identified as a *modified linear pairing-assignment problem* [32]. This formulation provides freedom to welcome the non-integer relaxed values for $\hat{\mathbf{\Phi}}, \hat{\mathbf{\Omega}}$ and $\hat{\mathbf{\Lambda}}$. However, we prove that the optimal subcarrier allocation and pairing policies of the relaxed problem always acquire an integer solution. For this, we provide the following theorem.

Definition 4 (Total-Unimodularity): A matrix *X* to be defined as a absolutely unimodular, with full row rank, if it satisfies the following two conditions: 1) each and every square sub-matrices of *X* follows $|X| = \{-1, 0, +1\}$ and 2) every single entry of *X* is an integer.

Theorem 3: For any continuous sequence bearing constraints of the form $Ax = v$, will consistently have an integer optimal solution if the constraint matrix *A* is entirely-unimodular and the vector demonstrated by *v* is an integer, respectively.

Proof: The proof is similar to [33] Appendix C, and is omitted here for brevity. ■

For optimal $(\hat{\boldsymbol{P}}_{\mathrm{S}}^\star, \hat{\boldsymbol{P}}_{\mathrm{R}}^\star, \hat{\mathbf{\Phi}}^\star, \hat{\mathbf{\Omega}}^\star, \hat{\mathbf{\Lambda}}^\star, \mathbf{\Sigma}^\star)$ and fixed EHTS time block $\boldsymbol{\alpha}$, the Lagrangian multipliers $(\lambda, \boldsymbol{\varphi}, \boldsymbol{\chi})$ are updated by applying subgradient method [26] as follows

$$\lambda(u+1) = \left[\lambda(u)+\epsilon_\lambda\left(\sum\nolimits_{k=1}^{K}\sum\nolimits_{m=1}^{N_{sc}}e^{\hat{P}^{m^\star}_{\mathrm{S}_k}}-P_{\max}\right)\right]^{+} \tag{36}$$

$$\varphi_j(u+1) = \left[\varphi_j(u)+\epsilon_\varphi\left(\sum\nolimits_{m=1}^{N_{sc}}\sum\nolimits_{n=1}^{N_{sc}}\hat{\Omega}_j^{m,n^\star}\hat{\Phi}^{m,n^\star}\times\frac{\left(1-\alpha_j^m\right)}{2}e^{\hat{P}^{n^\star}_{\mathrm{R}_j}}+\mathcal{M}_j^\star P_Q-\Sigma_j^\star\right)\right]^{+} \tag{37}$$

$$\chi_j(u+1) = \left[\chi_j(u)+\epsilon_\chi\left(\sum\nolimits_{m=1}^{N_{sc}}\hat{\mathbb{E}}^{m^\star}_{\mathrm{h}_j}-\Sigma_j^\star\right)\right]^{+} \tag{38}$$

where $\epsilon_\lambda, \epsilon_\varphi, \epsilon_\chi$ are positive step sizes, respectively. Similar to solving (**OP2a**), we take the partial derivative of the Lagrangian function of (**OP2b**) with respect to $\hat{\alpha}_j^m$ and setting the gradient to zero, we can obtain the optimal EHTS time block at the $(u+1)$-th iteration, owing to linear equation EHTS time block is updated as (39), as shown at the bottom of the next page. The corresponding Lagrangian multiplier is updated as

$$\nu_j(u+1) = \left[\nu_j(u)+\epsilon_\nu\left(\sum\nolimits_{m=1}^{N_{sc}}\sum\nolimits_{n=1}^{N_{sc}}\hat{\Omega}_j^{m,n^\star}\hat{\Phi}^{m,n^\star}\times\frac{\left(1-\alpha_j^m\right)}{2}e^{\hat{P}^{n^\star}_{\mathrm{R}_j}}+\mathcal{M}_j^\star P_Q-\sum\nolimits_{m=1}^{N_{sc}}\bar{\mathbb{E}}_{j,\Sigma}^{h^{m^\star}}\right)\right]^{+}, \tag{40}$$

where ϵ_α in (39) and ϵ_ν in (40) are positive step sizes.

Now, we propose the theorems for convergence of the SCA coefficients and the penalty factor.

Theorem 4: Let $\hat{\Upsilon}_{k,j}^{m,n^\star}(l)$ be the optimal solution for (**OP2a**) with the lower bound coefficients $(\gamma_{k,j}^{m,n}(l), \delta_{k,j}^{m,n}(l))$ at the l^{th} iteration. Then, if the coefficients are updated as

$$\gamma_{k,j}^{m,n}(l+1) = \frac{\hat{\Upsilon}_{k,j}^{m,n^\star}(l)}{1+\hat{\Upsilon}_{k,j}^{m,n^\star}(l)} \tag{41}$$

$$\delta_{k,j}^{m,n}(l+1) = \log_2\Big(1+\hat{\Upsilon}_{k,j}^{m,n^\star}(l)\Big) - \gamma_{k,j}^{m,n}(l+1)\log_2\Big(\hat{\Upsilon}_{k,j}^{m,n^\star}(l)\Big). \tag{42}$$

then the optimal value of $\hat{\varepsilon}(\boldsymbol{\alpha}, \hat{\boldsymbol{P}}_{\text{S}}, \hat{\boldsymbol{P}}_{\text{R}}, \hat{\boldsymbol{\Phi}}, \hat{\boldsymbol{\Omega}}, \hat{\boldsymbol{\Lambda}}, \boldsymbol{\gamma}, \boldsymbol{\delta})$ is monotonically increasing with l. Further, when the coefficients $\{\gamma_{k,j}^{m,n}(l), \delta_{k,j}^{m,n}(l)\}$ has converged, the optimal solution for **(OP2a)** and **(OP2b)** behaves as the local maximizer for the problem **(OP1)**.

Proof: The proof is similar to [7] Appendix A, and is omitted here for brevity. ∎

Proposition 3: For fixed EHTS time block $\boldsymbol{\alpha}(l)$, if the penalty factor Ψ is updated for the local maximizer $(\hat{\boldsymbol{P}}_{\text{S}}^\star(l), \hat{\boldsymbol{P}}_{\text{R}}^\star(l), \hat{\boldsymbol{\Phi}}^\star(l), \hat{\boldsymbol{\Omega}}^\star(l), \hat{\boldsymbol{\Lambda}}^\star(l), \boldsymbol{\Sigma}^\star(l))$ of (**OP2a**) at the l^{th} iteration as

$$\Psi(l+1) = \frac{\hat{\mathcal{R}}_T\Big(\boldsymbol{\alpha}(l), \hat{\boldsymbol{P}}_{\text{S}}^\star(l), \hat{\boldsymbol{P}}_{\text{R}}^\star(l), \hat{\boldsymbol{\Phi}}^\star(l), \hat{\boldsymbol{\Omega}}^\star(l), \hat{\boldsymbol{\Lambda}}^\star(l)\Big)}{\hat{\mathcal{P}}_T\Big(\hat{\boldsymbol{P}}_{\text{S}}^\star(l), \hat{\boldsymbol{P}}_{\text{R}}^\star(l), \hat{\boldsymbol{\Phi}}^\star(l), \hat{\boldsymbol{\Omega}}^\star(l), \hat{\boldsymbol{\Lambda}}^\star(l)\Big)} \tag{43}$$

then the penalty factor Ψ monotonically increases with l and we get $\Psi^\star = \lim_{l\to\infty}\Psi(l)$.

Proof: The proof is relegated to Appendix D. ∎

The static power dissipation plays a vital role in determining the system performance of the network, and we propose the following theorem for the same.

Theorem 5: The following properties are observed with static power P_C and P_Q.

1) For a given optimal resource allocation policy $(\boldsymbol{\alpha}, \hat{\boldsymbol{P}}_{\text{S}}^\star, \hat{\boldsymbol{P}}_{\text{R}}^\star, \hat{\boldsymbol{\Phi}}^\star, \hat{\boldsymbol{\Omega}}^\star, \hat{\boldsymbol{\Lambda}}^\star)$, with increasing static power dissipation (P_C, P_Q) maximum achievable optimal $\text{EE}^\star$ strictly decreases.
2) With increasing static power dissipation (P_C, P_Q) the optimal transmission power $(\hat{\boldsymbol{P}}_{\text{S}}^\star, \hat{\boldsymbol{P}}_{\text{R}}^\star)$ also strictly increases.

Proof: The proof is similar to [33] Appendix D, and is omitted here for brevity. ∎

Corollary 1: Directly implying from Theorem 6, as the relay static power P_Q increases, the probability of number of relays harvesting the power required for static power dissipation and transmission decreases, therefore the total number of relays selected $\mathcal{C}$ also decreases.

Algorithm 1 Iterative EEM Algorithm

1: Set the maximum number of iterations I_{max_1} and initialize the iteration counter $l=0$ and network penalty $\Psi(l)=0.001$.
2: **repeat** (Outer Loop)
3: Set the maximum number of iterations I_{max_2} and the step sizes $\epsilon_\lambda, \epsilon_\varphi, \epsilon_\chi$ and ϵ_ν;
4: Initialize iteration counter $v=0$, $\gamma_{k,j}^{m,n}(v)=1$, $\Sigma_j(v)=\infty$ and $\delta_{k,j}^{m,n}(v)=0$ and $\lambda(v), \boldsymbol{\varphi}(v), \boldsymbol{\chi}(v), \boldsymbol{\mu}(v)$ and $\boldsymbol{\nu}(v)$.
5: **repeat** (Inner Loop)
6: Update $\hat{P}_{\text{S}_k}^m$ and $\hat{P}_{\text{R}_j}^n$ using (27) and (28).
7: Update α_j^m using (6c).
8: Update $\boldsymbol{\Lambda}, \boldsymbol{\Omega}$ and $\boldsymbol{\Phi}$ using (31), (35) and $\Phi_{k,j}^{m,n^\star} = \max_{k,j}\Delta_{k,j}^{m,n},\ \forall k,j,m,n$ for (**OP7**) problem.
9: Update $\lambda(v), \boldsymbol{\varphi}(v), \boldsymbol{\chi}(v)$ and $\boldsymbol{\nu}(v)$ using (36), (37), (38) and (40).
10: Update $\gamma_{k,j}^{m,n}(v+1)$ and $\delta_{k,j}^{m,n}(v+1)$ using (41) and (42).
11: Set *counter* $=0$, $\mathcal{M}=0$ ▷ Calculating $\mathcal{M}$
12: **for** *counter* $<=$ *M* **do**
13: $\mathbf{M} = \hat{\boldsymbol{\Omega}}\hat{\boldsymbol{\Phi}}$ where $\mathbf{M} \in \mathbb{R}^{[N_{sc}\times N_{sc}\times M]}$
14: **if** $\sum_{j=1}^{N_{sc}}\sum_{k=1}^{N_{sc}}\mathbf{M}(j,k,counter) \geq 1$
15: $\mathcal{M} = \mathcal{M}+1$
16: **end if**
17: **end for** ▷ $\mathcal{C} = \sum_{j=1}^{J}\mathcal{M}_j$
18: **until** convergence to optimal solutions $\Big(\hat{\mathbf{P}}_S^\star, \hat{\mathbf{P}}_R^\star, \boldsymbol{\Sigma}^\star, \boldsymbol{\alpha}^\star, \boldsymbol{\Lambda}^\star, \boldsymbol{\Omega}^\star, \boldsymbol{\Phi}^\star\Big)$.
19: Set $\hat{P}_{\text{S}_k}^m(v+1) \leftarrow \hat{P}_{\text{S}_k}^{m^\star}, \hat{P}_{\text{R}_j}^n(v+1) \leftarrow \hat{P}_{\text{R}_j}^{n^\star}, \alpha_j^m(v+1) \leftarrow \alpha_j^{m^\star}, \Phi^{m,n}(v+1) \leftarrow \Phi^{m,n^\star}, \hat{\Lambda}_k^{m,n}(v+1) \leftarrow \hat{\Lambda}_k^{m,n^\star}$, $\hat{\Omega}_j^{m,n}(v+1) \leftarrow \hat{\Omega}_j^{m,n^\star}$ and update Σ_j using *Theorem 2*. Set $v \leftarrow v+1$.
20: Update $\Psi(l+1)$ using (43) and $l \leftarrow l+1$.
21: **until** convergence or $l > I_{max_1}$.

Corollary 2: Directly implying from Theorem 6, as the relay static power P_Q increases, the relay nodes with worse channel conditions try to harvest more energy to satisfy energy causality constraint (*C*.5). Thus the EHTS time block $\boldsymbol{\alpha}$ increases, without impacting the EE performance.

Next, we propose an iterative EEM algorithm and determine $\mathcal{M}$ with Algorithm 1, to find the near-optimal solution in order to maximize the EE of the network.

V. Model Extension

A. Suboptimal Algorithm for EHTS Protocol

The computational complexity of the proposed EEM algorithm under EHTS scenarios (as discussed in Section VI) increases significantly with N_{sc}. Thus, we propose a low-complexity suboptimal (SubOpt) algorithm for EHTS as described below:

Step 1 (Subcarrier Pairing for Fixed Power Allocation): In this step, we arrange the source-to-relay (SR) and the relay-to-destination (RD) subcarriers in the ascending order according to their respective channel gains and pair the corresponding subcarriers with each other in sequence, i.e., in a best-to-best and worst-to-worst fashion. Finally, the $N_{sc}\times N_{sc}$ matrix can

$$\hat{\alpha}_j^{m^\star}(u+1) = \Bigg[\hat{\alpha}_j^m(u) - \epsilon_\alpha\Bigg(\sum_{k=1}^{K}\sum_{j=1}^{J}\sum_{m=1}^{N_{sc}}\sum_{n=1}^{N_{sc}}\frac{\Phi_t^{m,n^\star}\hat{\Lambda}_{k,t}^{m,n^\star}\hat{\Omega}_j^{m,n^\star}}{2}\left(\frac{\gamma_{k,j}^{m,n}}{\ln(2)}\log\Big(\bar{\Upsilon}_{k,j}^{m,n^\star}\Big)+\delta_{k,j}^{m,n}\right) + \sum_{m=1}^{N_{sc}}\sum_{n=1}^{N_{sc}}\frac{\hat{\Omega}_j^{m,n^\star}\hat{\Phi}^{m,n^\star}}{2}e^{\hat{P}_{\text{R}_j}^{n^\star}} - \sum_{j=1}^{J}\sum_{m=1}^{N_{sc}}\sum_{k=1}^{K}\nu_j^\star\eta e^{\hat{P}_{\text{S}_k}^{m^\star}}\Big|h_{\text{S}_k\text{R}_j}^m\Big|^2\Bigg)\Bigg]^+ \tag{39}$$

be obtained as

$$\Phi^{m,n^\star} = \begin{cases} 1, & \text{for m-th subcarrier paired with n-th subcarrier} \\ 0, & \text{otherwise.} \end{cases} \tag{44}$$

Step 2 (Subcarrier Allocation for Fixed Power Allocation): Define $K \times (N_{sc} \times N_{sc})$ and $J \times (N_{sc} \times N_{sc})$ matrices for the k^{th} user pair and j^{th} relay node on the $(m,n)^{\text{th}}$ subcarrier pair. It is well-established that with AF relaying, the harmonic mean of the SNRs in first and second hop symbolizes the effective performance gains in the network. Inspired by this, we utilize this criteria for allocating the subcarriers to the users and relay nodes. Firlty, we describe the harmonic mean of the channels in both-hops for the given subcarrier pairing matrix $\mathbf{\Phi}$ below

$$\Theta_{k,j}^{m,n} = \frac{2\left|h_{\mathrm{S}_k\mathrm{R}_j}^{m} h_{\mathrm{R}_j\mathrm{D}_k}^{n}\right|^2}{\left|h_{\mathrm{S}_k\mathrm{R}_j}^{m}\right|^2 + \left|h_{\mathrm{R}_j\mathrm{D}_k}^{n}\right|^2}, \quad \forall\, k,j,(m,n) \tag{45}$$

Now, for the $(m,n)^{\text{th}}$ paired subcarrier we select the k^{th} user pair and j^{th} relay node that maximizes $\Theta_{k,j}^{m,n}$, also denoted by

$$\left\{\Lambda_k^{m,n^\star}, \Omega_j^{m,n^\star}\right\} = \begin{cases} 1, & \text{for } \{k,j\} = \arg\max_{k,j} \Theta_{k,j}^{m,n} \\ 0, & \text{otherwise, } \forall\,(m,n). \end{cases} \tag{46}$$

Step 3 (EHTS Time Block and Power Allocation): In the last step, the optimal power allocation $\mathbf{P}_S, \mathbf{P}_R$ can be found by solving the optimization problem (**OP3**) for the obtained $\mathbf{\Lambda}^\star, \mathbf{\Omega}^\star, \mathbf{\Phi}^\star$ in the step 1 and 2, respectively. Also, the EHTS time block $\boldsymbol{\alpha}$ for each relay node and subcarrier pair is kept to be equal, i.e., $\alpha_j^1 = \cdots = \alpha_j^m$, $\forall\, m,j$ and is searched between values {0.1, 0.2, 0.3, 0.4, 0.5, 0.6, 0.7, 0.8, 0.9} that satisfies the energy causality constraint (*C*.5). Lastly, the auxiliary variable $\mathbf{\Sigma}$ is updated using Theorem 2.

B. Best Relay Selection (BRS) Algorithm

To reduce the complexity of the proposed EEM algorithm, we propose a best relay selection (BRS) algorithm. Wherein the relay node with the best channel characterstics and maximum available harvested energy is selected for transmission. Firstly, we create a set $\mathcal{W}^{[1\times J]}$ for the relays satisfying the energy causality constraint (*C*.5), then we set $\mathcal{M}_j = 1$ if $j = \arg\max_{j\in W} \quad \hat{\varepsilon}(\boldsymbol{\alpha}, \hat{\boldsymbol{P}}_{\mathrm{S}}, \hat{\boldsymbol{P}}_{\mathrm{R}}, \hat{\mathbf{\Phi}}, \hat{\mathbf{\Omega}}, \hat{\mathbf{\Lambda}})$ and $\mathcal{M}_j = 0$, otherwise. For ease of mathematical representation, and maintaining the similarity to the proposed EEM algorithm, we set $\Omega_j^{m,n} = 1$ if $\mathcal{M}_j = 1$ and $\Omega_j^{m,n} = 0$, elsewhere. Then we implement the EEM resource allocation algorithm for BRS policy as described above by keeping the EHTS time block equal for each subcarrier, i.e., $\alpha_j^1 = \cdots = \alpha_j^m, \forall\, m$ whereas it vaires with each relay node. Directly, the optimal solution to the BRS algorithm can be obtained in a similar manner to the multi-relay selection strategy.

VI. Complexity Analysis

Let the number of power levels that taken by each $\hat{P}_{\mathrm{S}_k}^m$ and $\hat{P}_{\mathrm{R}_j}^n$ be denoted by Q. Moreover, the complexity of updating the dual variables is $\mathcal{O}((2KJ)^\varrho)$, where $\varrho = 2$ if the ellipsoid method is used [7]. Also, let the dual objective function in (**DP1**), the dual function for (**OP2b**) and the penalty factor Ψ converge in Z, Z'' and Z' iterations. We first introduce the understanding behind the complexity and then present the final complexity of all the algorithms in Table I.

- *EEM Algorithm:* In order to determine the optimal power allocation for *K* user pairs and *J* relay nodes with N_{sc} subcarriers in each hop, we need to solve $(K+J)N_{sc}^2$ subproblems. Each subcarrier pairing $\Phi^{m,n}$ is allocated to a particular user pair and relay node and each maximization in (31) and (35) has a complexity of $\mathcal{O}(KJ)$, hence the total complexity for subcarrier allocation to users and relays becomes $\mathcal{O}(KJN_{sc}^2)$. Further, the Hungarian method [32] is used to determine the optimal subcarrier pairing matrix with a complexity of $\mathcal{O}(N_{sc}^3)$. Therefore the total complexity for updating the dual variables for dual problem **(DP1)** is given by $\mathcal{O}(3(2KJ)^\varrho)$, and the complexity for solving the dual function for (**OP2b**) is $\mathcal{O}(2(2KJ)^\varrho)$.
- *ES Algorithm:* Let the number levels allowed for the EHTS time block α_j^m be *Y* and we follow the discussion from Section II-C.
- *SubOpt Algorithm:* Step 1 is used for subcarrier pairing has the additional complexity of $\mathcal{O}(2N_{sc})$ whereas in step 2 we traverese through a two-dimensional matrix of size $K \times J$ to obtain the subcarrier allocation and relay selection matrix together bringing the complexity of $\mathcal{O}((KJ)N_{sc})$. We follow the similar procedure as EEM for the optimal power and EHTS time block allocation is searched among the 9 possible values.
- *BRS Algorithm:* The total complexity of determining the optimal relay is now independent of the number of subcarriers in system, i.e., it becomes $\mathcal{O}(J)$, while the rest is similar to EEM. To compare the complexity of the proposed algorithms with the ES, we considered an example where $K = 2$, $J = 3$, $N_{sc} = 16$ as shown in the Table I and the proposed EEM method is $6.7856e + 23$ times faster than the ES. Also, the complexity analysis shows that SubOpt<BRS<EEM<ES on the scale of implementation cost.

VII. Simulation Results

In this section, we perform extensive computer simulations to exhibit the importance of energy-efficient designs and evaluate the performance gains for the proposed algorithms. We consider a practical 3GPP path loss model given by $131.1 + 42.8 \times \log_{10}(d)$ dB (d is in kilometres) [25]. Also, we employ i.i.d Rayleigh block fading effects $C\mathcal{N}(0,1)$ and log-normal shadowing $\sim \ln\mathcal{N}(0,4)$ dB for all the links in the network. The distance between user pairs is set as 25m and the relay nodes are deployed in the range of $1-2$m [5]. The subcarrier spacing and thermal noise density are given by 12 kHz and -174 dBm/Hz. Further, the static power dissipation for user nodes and relay nodes is taken as 10 mW [7] and 0.1 mW [5], [34]. Also, power harvesting and conversion efficiency is set as $\eta = 0.4$. The constant step sizes and penalty

TABLE I
COMPLEXITY ANALYSIS FOR DIFFERENT ALGORITHMS

Algorithm	**Complexity**
ES	$\mathcal{O}\left((K2^J-1)(KJ)^{N_{sc}}N_{sc}!(Q^3+2)+N_{sc}JY\right)$
Proposed EEM	$\mathcal{O}\left((2KJ)^{\varrho}\left(3ZZ'N_{sc}^2\left((K+J)(Q^3+2)+KJ+N_{sc}\right)+2Z''\right)\right)$
SubOpt	$\mathcal{O}\left(N_{sc}\left(K+J+2+3(2KJ)^{\varrho}ZZ'N_{sc}(KJ)(Q^3+2)\right)+9Z''\right)$
BRS	$\mathcal{O}\left((2KJ)^{\varrho}\left(3ZZ'N_{sc}^2\left((K+J)(Q^3+2)+K+N_{sc}\right)+2Z''+J\right)\right)$
Example	$K=2, J=5, N_{sc}=16, \varrho=2, Y=9, Q=10, Z=Z'=Z''=3$
ES/EEM	$1.3208e+34/1.9464e+10=6.7856e+23$
ES/BRS	$1.3208e+34/1.9442e+10=6.7934e+23$
ES/SubOpt	$1.3208e+34/1.9392e+10=6.8108e+23$

factor that gives trade-off between SE and EE are set to be 10^{-3} and 10^{-4}. The convergence tolerance value is 10^{-7}. As a benchmark, we compare the proposed EEM, SubOpt and BRS algorithms with ES and the following algorithms:

1) EEM with Equal EHTS time block - In this algorithm, the proposed EEM algorithms are implemented where each j^{th} relay node operates under the same EHTS time block over all the subcarriers allocated to that relay node, i.e., $\alpha_j^1=\cdots=\alpha_j^m, \forall\, m$.
2) Direct transmission (DT) - In this algorithm, we consider a direct transmission between the user nodes without subcarrier allocation.
3) EHPS regime (PSR) - As a benchmark, we also simulated EHPS scheme and compared it's performance with the EHTS. The transmission in EHPS protocol takes place in two phases, multiple access (MA) and broadcast (BC) phase. Firstly, in MA phase, the K source nodes transmit their intended signals to the J EH relay nodes, all of which harvests energy from procured RF signals employing EHPS protocol. Later in BC phase the *selected* relay node(s) broadcast the amplified signal(s) to the K destination nodes. Further, in the communication block time for EH and IF at the relay nodes employing EHPS protocol the total block time $\mathcal{T}$ is divided into two equal segments of $\mathcal{T}/2$. In the first block time, the procured power at j^{th} relay node and for m^{th} subcarrier is further divided in a ratio of ρ_j^m and $(1-\rho_j^m)$ for EH and signal transmission in MA phase, with $0\leq\rho_j^m\leq 1$. Note that the selection of the power ratio, ρ_j^m, used for EH at the j^{th} relay node on m^{th} subcarrier, creates a balance between EH and IF modes. The second segment of $\mathcal{T}/2$ block length is employed for signal transmission in BC phase. The optimal resource allocation policy can be obtained for EHPS.

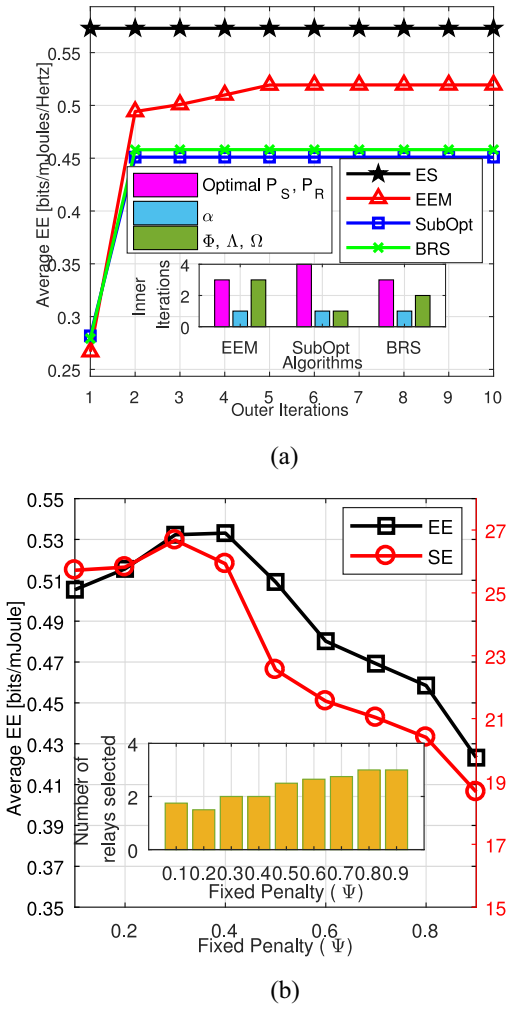

Fig. 4. Convergence behaviour of the proposed algorithms and effect of different network penalty on average SE and EE performance. (a) Convergence behavior of the proposed algorithms. (b) Penalty factor Ψ versus average SE and EE.

A. Convergence Behaviour and Effect of Network Penalty

We first take a look at the convergence of the proposed algorithms and the effect of penalty factor on the average SE and EE performance with $K=2$, $J=3$, $N_{sc}=8$, $P_{\max}=10$ dBm, d_{SR} is fixed at 2m. Fig. 4a demonstrates the convergence behaviour of the proposed algorithms for a *single channel realization*, clearly, the inner iterations for the proposed algorithms converge in the following order BRS=SubOpt<EEM. Also, the outer iterations of the proposed algorithms converge in less than seven iterations as detailed in Proposition 3. In Fig. 4a, it can be observed that the performance of the proposed EEM algorithm increases monotonically and after convergence, it's performance reaches closer to the optimal ES. Fig. 4b represents the effect of varying network penalty Ψ on the average SE and EE performance of the proposed EEM algorithm.

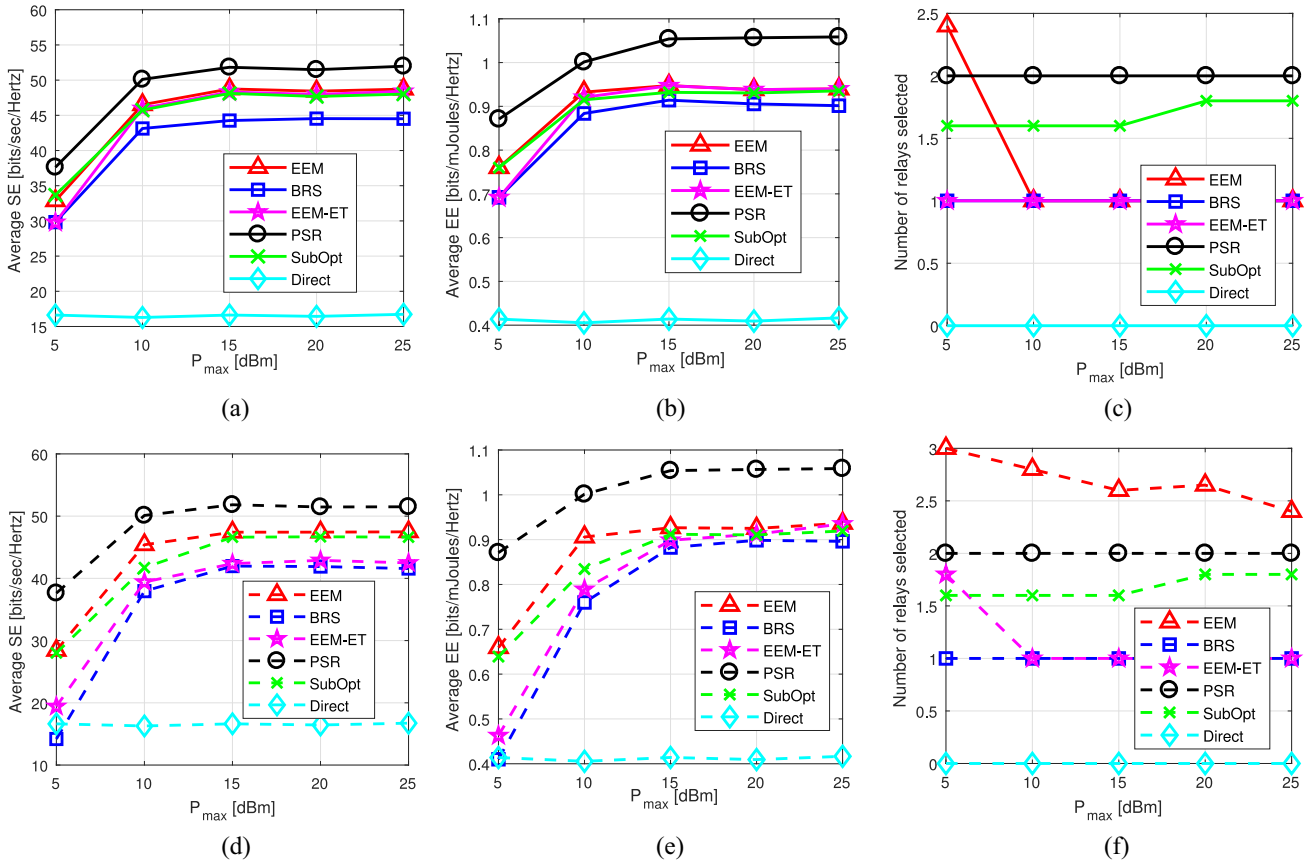

Fig. 5. Performance comparison of various algorithms where (a)-(c) represents for $d_{SR} = 1$m and (d)-(f) for $d_{SR} = 2$m. (a) Average SE versus P_{max}. (b) Average EE versus P_{max}. (c) Selected relays versus P_{max}. (d) Average SE versus P_{max}. (e) Average EE versus P_{max}. (f) Selected relays versus P_{max}.

TABLE II
CPU RUN-TIME (IN SECS) ANALYSIS FOR DIFFERENT ALGORITHMS FOR $K = 2, J = 3, P_{max} = 20$ dBm

Algorithm	ES	EEM	BRS	SubOpt
$N_{sc} = 4$	31104.743	140.457	136.349	126.217

Evidently, the average EE and SE performance first increases and then decreases, as the penalty increases, and the optimal (maximum) EE is achieved at $\Psi^{\star} = 0.4$. This is due to the fact that the SE increases on a log scale while the utilized network power increases linearly, thus the network penalty helps in establishing a trade-off between the SE and EE performance gains. Also, as the network penalty increases the average number of relay nodes selected also increases, leading to more power dissipation and thus we can see a decline in EE after $\Psi \geq 0.4$, respectively.

We compute the average CPU time (in seconds) for all the proposed and the ES algorithms depicted in the Table II. Clearly, our proposed algorithm takes significantly less time compared to the ES algorithm. Further, as indicated by the convergence figure, our proposed algorithm obtains the performance very near to the ES algorithm, and can be implemented in real-time.

Please note that all the algorithms are implemented on Intel Core i7-6700 processor with 3.40GHz clock and Intel HD Graphics 530 (Skylake GT2). The operating system is Ubuntu 16.04 LTS and 64 Gb memory.

B. Performance Comparison & Effect of Distance

Now, we demonstrate the performance comparison of various algorithms and the impact of distance, with $K = 2, J = 3$, $N_{sc} = 16$ when the relay nodes are placed at $d_{SR} = 1$m for Fig. 5a–5c and $d_{SR} = 2$m for Fig. 5d–5f. It is evident that the EHPS protocol outperforms the EHTS both in SE and EE performance because of the delay-limited transmission. This can be explained by the fact that the optimal value of $\boldsymbol{\alpha}$ increases by increasing $\sigma^{m^2}_{R_j}$ or $\sigma^{m^2}_{P_{R_j}}$. However, the optimal value of $\boldsymbol{\rho}$ increases by increasing antenna noise variance $\sigma^{m^2}_{R_j}$ and decreases by increasing processing noise variance $\sigma^{m^2}_{P_{R_j}}$. This is due to the fact that for EHTS protocol both noise processes, the antenna noise at the baseband $n^m_{R_j}$ and the conversion noise $n^m_{P_{R_j}}$, affect the received signal at relay in a similar fashion. On the other hand, for EHPS protocol, the baseband antenna noise $n^m_{R_j}$ affects the received signal at relay and the conversion noise $n^m_{P_{R_j}}$ affects the portion of the received signal strength $\sqrt{1-\rho^m_j}$ at the relay. Also, the positioning of relay nodes have almost no impact on EHPS performance and the average number of relay selected. Moreover, when the relay nodes are placed at 1m

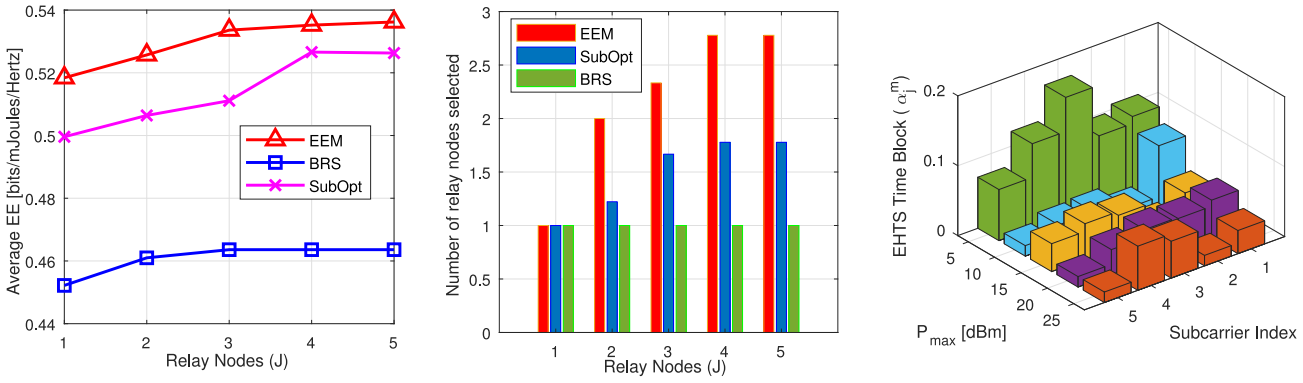

Fig. 6. Effect of Varying Relay Nodes and average optimal EHTS time-block. (a) Average EE versus J. (b) Average relay selected versus J. (c) EHTS time block ($\boldsymbol{\alpha}$).

(closer to the source nodes) then almost all the proposed algorithms behave very closely, whereas as the distance between the source and relay node increases to 2m the performance gap between the proposed EEM algorithm and other algorithm increases, this is due to the fact that EEM performs joint multi-parameter optimisation that control the EE of the network and the number of relay nodes selected at 1m approximately remains same compared to relays placed at 2m. Therefore, as the distance between the source nodes and relays increases the performance of the EEM algorithm compared to other algorithms increases because of optimal relay selection policy. Moreover, the average EE and SE increases for $P_{\max} \leq 15$ dBm and becomes constant at higher transmit power budget $P_{\max} \geq 15$ dBm. When operating in limited transmit power budget $P_{\max} \leq 15$ dBm we can see significant difference in the performance of EEM and other proposed algorithms indicating the importance of joint optimisation with EEM leading to a beter relay selection policy, whereas when the transmit power budget becomes rich $P_{\max} \geq 15$ dBm, then the performance of the other algorithms becomes comparable. Further, as the transmit power budget increases the average number of relays selected reduces, this is because the chances of satisfying the energy causality constraint by the relay node increases, even with channel deteriortions, thereby to lower the power dissipation lesser number of relays is selected as the budget becomes rich. Moreover, the equal EHTS time block scenario (EEM-ET) outperforms the BRS policy because of multi-relay selection policy and optimal designing of EHTS time block for EEM-ET. Also, EEM algorithm outperforms SubOpt, BRS and direct transmission (DT) algorithm due to higher cooperative diversity gain.

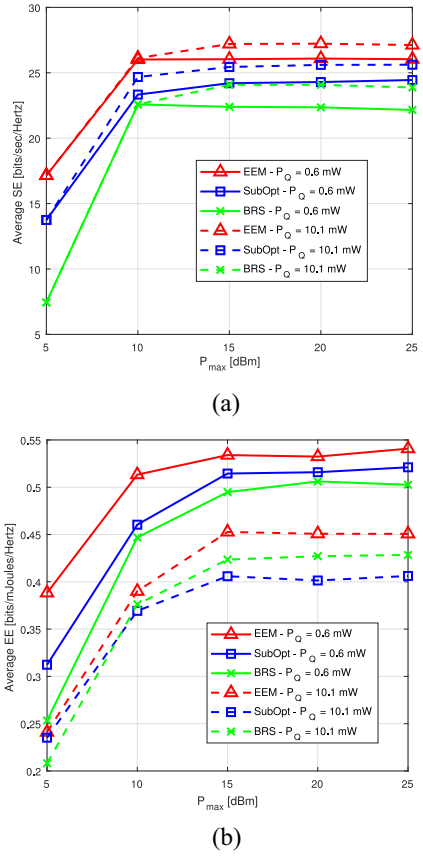

Fig. 7. Performance comparison of various relay static power dissipation. (a) Average SE versus P_{max}. (b) Average EE versus P_{max}.

C. Effect of Varying Relay Nodes

We now compare the performance of proposed algorithms with varying number of relay nodes in the network for $K = 2$, $J = \{1, \ldots, 5\}$, $N_{sc} = 8$, $P_{\max} = 15$ dBm, $d_{SD} = 45$m, when the relay nodes are placed randomly in the range of 2.5−3.5 m. It can be clearly seen from Fig. 6a that as the number of relay node increases the average EE performance improves rapidly for $J \leq 4$, whereas it becomes steady for $J > 4$. This is because we get higher cooperative diversity gain as the probability of selecting relay nodes increases. Further, as the number of relay nodes becomes $J > 4$ the performance saturates due to the limited number of subcarriers and power. To get better insights, we plot Fig. 6b that shows the average number of relays selected with varying number of relay nodes. we can observe that the total number of relays selected in EEM and SubOpt algorithm increases as the number of relay nodes increases and thus it helps in achieving higher cooperative diversity gain. In result, the EEM and SubOpt algorithms

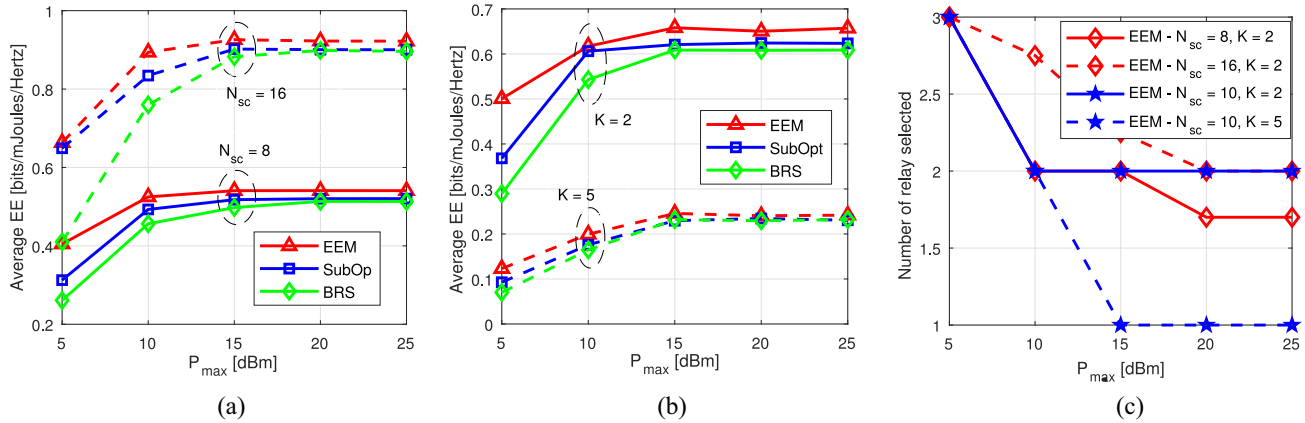

Fig. 8. Effect of varying available subcarriers and user pairs. (a) Effect of varying subcarriers. (b) Effect of varying user pairs. (c) Average number of relays selected.

outperform the BRS algorithm. Also, we show the optimal EHTS time block for $J = 1$, $K = 2$, $N_{sc} = 5$, $\eta = 0.3$, $d_{SD} = 20$m and $d_{SR} = 1$m in Fig. 6c. As expected the average EHTS time block decreases with increasing $P_{\max}$, because the source nodes can transmit with higher power levels. Moreover, each subcarrier is allocated with varying EHTS time block depending on the channel characteristics.

D. Effect of Static Power Dissipation

We now analyse the performance comparison with varying relay static power dissipation, with $K = 2$, $J = 3$, $Nsc = 8$, $P_Q = 0.6$, 10.1 mW. To model the high static power dissipation P_Q at relay nodes, we introduce an initially charged battery [19] at the relay nodes to satisfy the energy causality constraint (C.5), such that only 0.1 mW of static power (apart from the required relay transmission power) is needed to be harvested. As expected, we can clearly see that the SE and EE performance of the network saturates when the power budget becomes high $P_{max} \geq 15$ dBm due to SE-EE trade-off. Moreover, as the static power dissipation increases the EE of the network reduces, whereas, SE of the network increases, this occurs due to the fact that the model tries to allocate more power to the source nodes to satisfy the energy-causality constraint and this also leads to decreasing the EE, directly matching the analysis in *Theorem 8*. Moreover, EEM outperforms the BRS and SubOpt algorithms, due to the fact that it determines the most optimal relay selection policy for the network.

E. Effect of Varying Available Subcarriers and User Pairs

Fig. 8a demonstrates the performance comparison of varying subcarriers versus source transmit power budget, with $K = 2$, $J = 3$, $N_{sc} = \{8, 16\}$ and $d_{SR} = 2$m. It can be observed that the average EE performance of the proposed algorithms increases significantly as $P_{\max}$ increases and it becomes steady after $P_{\max} \geq 15$ dBm. Also, the average EE performance of the proposed algorithms increase swiftly as N_{sc} increases, as expected due to frequency diversity. Moreover, as the number of subcarrier increases the performance gap between the EEM and other algorithm also increases, especially in limited power budget $P_{max} \leq 15$ dBm. Moreover, Fig. 8b indicates the performance comparison of varying user pairs versus source transmit power budget, with $K = \{2, 5\}$, $J = 3$, $N_{sc} = 10$ and $d_{SR} = 2$m. As can be seen, as the K increases the average EE performance deteriorates due to monotonic increase in the static power of the network. As expected, the performance of the proposed algorithms is in the order EEM>SubOpt>BRS. Further, the performance gap between EEM and other proposed algorithm is greater in low transmit power budget for $K = 2$ as compared to $K = 5$ in Fig. 8b, because of the limited number of subcarriers. Directly, as depicted by Fig. 8c, as the number of subcarriers increases, the average number of selected relay node increases, whereas with the increase in the number of user pairs in the network, the number of relays selected reduces, this is due to the fact that the model tries to minimize the total power consumption.

VIII. Conclusion and Future Works

In this work we formulated a joint multi-relay selection and multi-parameter EEM optimisation problem for multi-user multi-carrier AF network under EHTS SWIPT paradigm, that was transformed to a tractable quasi-concave form. Based on the dual decomposition, we proposed an iterative EEM algorithm. Further, a low-complexity SubOpt and BRS algorithms were investigated. The proposed algorithms outperform benchmark algorithms like the equal alpha allocation, DT algorithms. The performance of the EEM and SubOpt algorithm improves significantly compared to the BRS algorithm when operating in limited transmission power budget. Further we established the relationship between network penalty Ψ and the SE and EE performance gains. Moreover, we manifested that designing an optimal EHTS time block for each subcarrier ameliorates the performance gains, by comparing the proposed models with equal alpha algorithm. In addition, we demonstrated the impact of various network parameters on the SE and EE performance of the system such as number of relay nodes, number of subcarriers and number of relay nodes. In conclusion, this work provides an in-depth analysis to enable the practical deployment of power-constrained sensor nodes employing SWIPT paradigm. We will analyse

energy-constrained MIMO relay network under imperfect CSI and extend the model for multiple time slots and EHPS SWIPT network in the future work.

APPENDIX A
PROOF OF THEOREM 1

The lower bound for (**OP2a**) and (**OP2b**) can be given directly by $\hat{\mathcal{R}}_T$ and $\dot{\mathcal{R}}_T$. Also, $\log(\hat{\Upsilon}_{k,j}^{m,n})$ and $\log(\hat{\Upsilon}_{k,j}^{m,n})$ can be derived as $\log(\hat{\Upsilon}_{k,j}^{m,n}) = \hat{P}_{\mathrm{R}_j}^n + \hat{P}_{\mathrm{S}_k}^m + \log(|h_{\mathrm{S}_k\mathrm{R}_j}^m h_{\mathrm{R}_j\mathrm{D}_k}^n|^2) - \log\big[|h_{\mathrm{R}_j\mathrm{D}_k}^n|^2 e^{\hat{P}_{\mathrm{R}_j}^n}(\sum_{l\neq k}^K e^{\hat{P}_{\mathrm{S}_l}^m}|h_{\mathrm{S}_l\mathrm{R}_j}^m|^2 + \sigma_{S_{\mathrm{R}_j}}^{m^2}) + \sigma_{\mathrm{D}_k}^{n^2}(\sum_{k=1}^K e^{\hat{P}_{\mathrm{S}_k}^m}|h_{\mathrm{S}_k\mathrm{R}_j}^m|^2 + \sigma_{S_{\mathrm{R}_j}}^{m^2})\big]$ and $\log(\hat{\Upsilon}_{k,j}^{m,n}) = \hat{P}_{\mathrm{R}_j}^n + \hat{P}_{\mathrm{S}_k}^m + \log|h_{\mathrm{S}_k\mathrm{R}_j}^m h_{\mathrm{R}_j\mathrm{D}_k}^n|^2 - \log\big[|h_{\mathrm{R}_j\mathrm{D}_k}^n|^2 e^{\hat{P}_{\mathrm{R}_j}^n}(\sum_{l\neq k}^K e^{\hat{P}_{\mathrm{S}_l}^m}|h_{\mathrm{S}_l\mathrm{R}_j}^m|^2 + \hat{\sigma}_{S_{\mathrm{R}_j}}^{m^2}) + \sigma_{\mathrm{D}_k}^{n^2}(\sum_{k=1}^K e^{\hat{P}_{\mathrm{S}_k}^m}|h_{\mathrm{S}_k\mathrm{R}_j}^m|^2 + \hat{\sigma}_{S_{\mathrm{R}_j}}^{m^2})\big]$. Since $\{\gamma_{k,j}^{m,n} \geq 0, \delta_{k,j}^{m,n} \geq 0, \Psi\} \geq 0$ and fixed $(\hat{\Phi}^{m,n}\hat{\Lambda}_k^{m,n}\hat{\Omega}_j^{m,n})$, the concavitiy of the lower bounds for (**OP2a**) and (**OP2b**) follow from the summation of affine and concave terms (i.e., log-sum-exp terms and minus-exp terms [26]) and thus problems are quasi-concave [26].

APPENDIX B
PROOF OF PROPOSITION 1

As our first step, we show that within polynomial time an arbitrary instance of SS is converted to a special instance of EEM optimization problem [36]. For example, consider a target V and the arbitrary instance of SS along with the natural numbers set given by $\mathcal{W} = w_l$. Now, we design a two-relay and two-user EEM instance below. Conditioned on the energy-causality constraint for each relay node, for each natural number w_l, we design a subcarrier l such that its rate-power function remains equal for both the users for each EH relay node. Therefore, the power required for EE 0 is 0, the power for EE w_l is $P/|\mathcal{W}|$ and EE keeps increasing to a point, suppose the power for EE $w_l + 1/|\mathcal{W}|$ at that point is P after which it starts declining. We assert that, by taking into account of the two-EH relay nodes and two-user pairs, SS has a satisfying solution if : (1) a policy for subcarrier allocation and pairing exists, such that the EE request of each user pair is given by V and $\sum_{l=1}^b w_l - V$ [36], (2) the selected EH relay node(s) satisfies the energy causality constraint, and (3) the total power consumption is not exceeded.

Suppose, a solution of SS is of the form that sum of the subset Q totals to V [36]. Assuming, EH relay nodes' energy causality constraint is satisfied with the received power, if each of the subcarrier present in the subset Q is allocated to the first user and first EH relay node, whereas the rest of the subcarriers are allocated to the second user and second EH relay node, respectively. Moreover, we add an EE load of w_l on every subcarrier, therefore it will lead to an optimally satisfying solution to the problem (**OP2a**). But if Q is not there, leading to no subset summing exactly to V. It is to be noted that the difference of V and the sum of a subset at any given time, should always be greater or equal to 1. Moreover, the maximum number of subcarriers that can be allocated to individual user pairs and relay nodes is constrained by $|\mathcal{W}| - 1$. Directly from [36], it will lead to a condition wherein the EH relay nodes and the user nodes has to load a minimum of one assigned subcarrier with EE greater than $w_l + 1/|\mathcal{W}|$, leading to the exceeding of the total power budget (P).

APPENDIX C
PROOF OF PROPOSITION 2

The objective function of the optimization problem (**OP2a**) can be reformulated and is given in (C.1), as shown at the top of the next page, where $\{\boldsymbol{\alpha}, \hat{\boldsymbol{P}}_{\mathrm{S}}, \hat{\boldsymbol{P}}_{\mathrm{R}}\} \in \mathbb{W}^{K\times J}$ and $\Pi_{m,n}(\cdot) : \mathbb{W}^{K\times J} \to \mathbb{R}$ with its convexity not gauranteed. In a similar way, the constraints (C.1)−(C.8) can also be modified as $\sum_{m=1}^{N_{sc}}\sum_{n=1}^{N_{sc}} \Theta_{m,n}(\boldsymbol{\alpha}, \hat{\boldsymbol{P}}_{\mathrm{S}}, \hat{\boldsymbol{P}}_{\mathrm{R}}, \boldsymbol{\Sigma}, \boldsymbol{\gamma}, \boldsymbol{\delta}) \leq 0$, where $\Theta_{m,n}(\cdot) : \mathbb{W}^{K\times J} \to \mathbb{R}^7$, and we elaborate the transformations given below

$$(TF1) \quad \max_{\hat{\boldsymbol{P}}_{\mathrm{S}}, \hat{\boldsymbol{P}}_{\mathrm{R}}} \quad \sum_{m=1}^{N_{sc}}\sum_{n=1}^{N_{sc}} \Pi_{m,n}\Big(\boldsymbol{\alpha}, \hat{\boldsymbol{P}}_{\mathrm{S}}, \hat{\boldsymbol{P}}_{\mathrm{R}}\Big)$$
$$\text{subject to } \sum_{m=1}^{N_{sc}}\sum_{n=1}^{N_{sc}} \Theta_{m,n}\Big(\boldsymbol{\alpha}, \hat{\boldsymbol{P}}_{\mathrm{S}}, \hat{\boldsymbol{P}}_{\mathrm{R}}, \boldsymbol{\Sigma}, \boldsymbol{\gamma}, \boldsymbol{\delta}\Big) \leq x \tag{C.2}$$

where x indicates a variable $x \in \mathbb{R}^7$. Moreover, we can now obtain (**OP3**) by transforming the optimization problem, i.e., by substituting $x = 0$ in **(TF1)**, moreover for the perturbation vector Q, we can assign $x = Q$ and obtain the perturbation function $\Upsilon(Q)$. It is established from [30] that the duality gap plummets to zero if we satisfy the time-sharing condition. Also, it further establishes that if the procured optimal solution of the optimisation problem (**OP3**) is a concave function of the constraints then the time-sharing condition is satisfied [30]. Therefore, the duality gap tends to be zero, when $\Upsilon(Q)$ becomes a concave function in Q. Hence, we follow the three step approach stated below.

Step 1 - (Procuring the Time-Sharing Property): If $\{\hat{\boldsymbol{P}}_{\mathrm{S}}, \hat{\boldsymbol{P}}_{\mathrm{R}}\}$, $k = 1, 2$ and $j = 1, 2$ whilst the relay nodes are taken from the set $\Re = \{1, 2, \{1, 2\}\}$. Suppose both the relay nodes are selected, i.e., from the set {1, 2} thereby the optimal solutions of (**OP3**) is given by $\Upsilon(Q_1)$ and $\Upsilon(Q_2)$, hence a solution $\{\hat{P}_{\mathrm{S}_3}^{m^\star}, \hat{P}_{\mathrm{R}_1}^{n^\star}, \hat{P}_{\mathrm{R}_2}^{n'^\star}\}$ always exists, wherein n^{th} subcarrier is assigned to the 1^{st} relay and n' to the 2^{nd} relay, for $0 \leq \Delta \leq 1$, such that

$$\sum_{m=1}^{N_{sc}}\sum_{n=1}^{N_{sc}} \Theta_{m,n}\Big(\boldsymbol{\alpha}, \hat{P}_{\mathrm{S}_3}^{m^\star}, \hat{P}_{\mathrm{R}_1}^{n^\star}, \hat{P}_{\mathrm{R}_2}^{n'^\star}, \boldsymbol{\Sigma}, \boldsymbol{\gamma}, \boldsymbol{\delta}\Big) \leq \Delta Q_1 + (1-\Delta)Q_2 \tag{C.3}$$

$$\sum_{m=1}^{N_{sc}}\sum_{n=1}^{N_{sc}} \Pi_{m,n}\Big(\boldsymbol{\alpha}, \hat{P}_{\mathrm{S}_3}^{m^\star}, \hat{P}_{\mathrm{R}_1}^{n^\star}, \hat{P}_{\mathrm{R}_2}^{n'^\star}\Big) \geq \Delta \sum_{m=1}^{N_{sc}}\sum_{n=1}^{N_{sc}} \Pi_{m,n}\Big(\boldsymbol{\alpha}, \hat{P}_{\mathrm{S}_1}^{m^\star}, \hat{P}_{\mathrm{R}_1}^{n^\star}, \hat{P}_{\mathrm{R}_2}^{n'^\star}\Big) + (1-\Delta)\sum_{m=1}^{N_{sc}}\sum_{n=1}^{N_{sc}} \Pi_{m,n}\Big(\boldsymbol{\alpha}, \hat{P}_{\mathrm{S}_2}^{m^\star}, \hat{P}_{\mathrm{R}_1}^{n^\star}, \hat{P}_{\mathrm{R}_2}^{n'^\star}\Big). \tag{C.4}$$

Step 2 - (Proving Concavity of $\Upsilon(Q)$): Suppose we have Δ, then we can easily mandate that Q_3 satisfies $Q_3 = \Delta Q_1 + (1-\Delta)Q_2$. If $\{\boldsymbol{\alpha}, \hat{P}_{\mathrm{S}_1}^{m^\star}, \hat{P}_{\mathrm{R}_1}^{n^\star}, \hat{P}_{\mathrm{R}_2}^{n'^\star}\}$, $\{\boldsymbol{\alpha}, \hat{P}_{\mathrm{S}_2}^{m^\star}, \hat{P}_{\mathrm{R}_1}^{n^\star}, \hat{P}_{\mathrm{R}_2}^{n'^\star}\}$ and $\{\boldsymbol{\alpha}, \hat{P}_{\mathrm{S}_3}^{m^\star}, \hat{P}_{\mathrm{R}_1}^{n^\star}, \hat{P}_{\mathrm{R}_2}^{n'^\star}\}$ are the optimal solutions governed by the constraints $\Upsilon(Q_1), \Upsilon(Q_2)$ and $\Upsilon(Q_3)$, then with the help of the time sharing property we obtain

$$\hat{\varepsilon}\Big(\boldsymbol{\alpha},\hat{\boldsymbol{P}}_{\rm S},\hat{\boldsymbol{P}}_{\rm R},\hat{\boldsymbol{\Phi}},\hat{\boldsymbol{\Omega}},\hat{\boldsymbol{\Lambda}}\Big)=\sum\nolimits_{m=1}^{N_{sc}}\sum\nolimits_{n=1}^{N_{sc}}\Bigg(\sum\nolimits_{k=1}^{K}\sum\nolimits_{j=1}^{J}\frac{(1-\alpha_j^m)}{2}\hat{\Phi}^{m,n}\hat{\Lambda}_k^{m,n}\hat{\Omega}_j^{m,n}\Bigg(\frac{\gamma_{k,j}^{m,n}}{\ln(2)}\ln\Big(\hat{\Upsilon}_{k,j}^{m,n}\Big)+\delta_{k,j}^{m,n}\Bigg)$$
$$-\Psi\Bigg(\sum\nolimits_{k=1}^{K}\sum\nolimits_{j=1}^{J}\hat{\Phi}^{m,n}\hat{\Lambda}_k^{m,n}\hat{\Omega}_j^{m,n}\Big(e^{\hat{P}_{{\rm S}_k}^m}+e^{\hat{P}_{{\rm R}_j}^n}\Big)+\frac{2KP_C+\mathcal{C}P_Q}{N_{sc}^2}\Bigg)\Bigg)=\sum\nolimits_{m=1}^{N_{sc}}\sum\nolimits_{n=1}^{N_{sc}}\Pi_{m,n}\Big(\boldsymbol{\alpha},\hat{\boldsymbol{P}}_{\rm S},\hat{\boldsymbol{P}}_{\rm R}\Big) \quad \text{(C.1)}$$

$$\mathcal{G}(\Psi(l))\geq\hat{\mathcal{R}}_T\Big(\boldsymbol{\alpha}^\star(l),\hat{\boldsymbol{P}}_{\rm S}^\star(l-1),\hat{\boldsymbol{P}}_{\rm R}^\star(l-1),\hat{\boldsymbol{\Phi}}^\star(l-1),\hat{\boldsymbol{\Omega}}^\star(l-1),\hat{\boldsymbol{\Lambda}}^\star(l-1)\Big)$$
$$-\ \Psi(l)\hat{\mathcal{P}}_T\Big(\hat{\boldsymbol{P}}_{\rm S}^\star(l-1),\hat{\boldsymbol{P}}_{\rm R}^\star(l-1),\hat{\boldsymbol{\Phi}}^\star(l-1),\hat{\boldsymbol{\Omega}}^\star(l-1),\hat{\boldsymbol{\Lambda}}^\star(l-1)\Big) \quad \text{(D.2)}$$

$$\mathcal{G}(\Psi(l))=\hat{\mathcal{R}}_T\Big(\boldsymbol{\alpha}^\star(l),\hat{\boldsymbol{P}}_{\rm S}^\star(l),\hat{\boldsymbol{P}}_{\rm R}^\star(l),\hat{\boldsymbol{\Phi}}^\star(l),\hat{\boldsymbol{\Omega}}^\star(l),\hat{\boldsymbol{\Lambda}}^\star(l)\Big)-\Psi(l)\hat{\mathcal{P}}_T\Big(\hat{\boldsymbol{P}}_{\rm S}^\star(l),\hat{\boldsymbol{P}}_{\rm R}^\star(l),\hat{\boldsymbol{\Phi}}^\star(l),\hat{\boldsymbol{\Omega}}^\star(l),\hat{\boldsymbol{\Lambda}}^\star(l)\Big)$$
$$=\hat{\mathcal{P}}_T\Big(\hat{\boldsymbol{P}}_{\rm S}^\star(l),\hat{\boldsymbol{P}}_{\rm R}^\star(l),\hat{\boldsymbol{\Phi}}^\star(l),\hat{\boldsymbol{\Omega}}^\star(l),\hat{\boldsymbol{\Lambda}}^\star(l)\Big)(\Psi(l+1)-\Psi(l))\geq 0 \quad \text{(D.3)}$$

$\{\boldsymbol{\alpha},\hat{P}_{\rm S_3}^{m^\star},\hat{P}_{\rm R_1}^{n^\star},\hat{P}_{\rm R_2}^{n'^\star},\boldsymbol{\Sigma},\boldsymbol{\gamma},\boldsymbol{\delta}\}$ satisfying (C.3) and (C.4). Therefore, $\{\boldsymbol{\alpha},\hat{P}_{\rm S_3}^{m^\star},\hat{P}_{\rm R_1}^{n^\star},\hat{P}_{\rm R_2}^{n'^\star}\}$ becomes the optimal solution of $\Upsilon(Q_3)$, giving

$$\sum\nolimits_{m=1}^{N_{sc}}\sum\nolimits_{n=1}^{N_{sc}}\Pi_{m,n}\Big(\boldsymbol{\alpha},\hat{P}_{\rm S_3}^{m^\star},\hat{P}_{\rm R_1}^{n^\star},\hat{P}_{\rm R_2}^{n'^\star}\Big)$$
$$\geq\Delta\sum\nolimits_{m=1}^{N_{sc}}\sum\nolimits_{n=1}^{N_{sc}}\Pi_{m,n}\Big(\boldsymbol{\alpha},\hat{P}_{\rm S_1}^{m^\star},\hat{P}_{\rm R_1}^{n^\star},\hat{P}_{\rm R_2}^{n'^\star}\Big)$$
$$+\ (1-\Delta)\sum\nolimits_{m=1}^{N_{sc}}\sum\nolimits_{n=1}^{N_{sc}}\Pi_{m,n}\Big(\boldsymbol{\alpha},\hat{P}_{\rm S_2}^{m^\star},\hat{P}_{\rm R_1}^{n^\star},\hat{P}_{\rm R_2}^{n'^\star}\Big). \quad \text{(C.5)}$$

*Step 3 - Proving Time-Sharing Property Is Satisfied by (**OP3**):* It is evident from [32], that as the total number of subcarriers approaches to infinity the time-sharing condition always holds true. Suppose $\{\boldsymbol{\alpha},\hat{P}_{\rm S_1}^{m^\star},\hat{P}_{\rm R_1}^{n^\star},\hat{P}_{\rm R_2}^{n'^\star}\}$ and $\{\boldsymbol{\alpha},\hat{P}_{\rm S_2}^{m^\star},\hat{P}_{\rm R_1}^{n^\star},\hat{P}_{\rm R_2}^{n'^\star}\}$ be two feasible solutions with $\Delta\times N_{sc}$ and $(1-\Delta)\times N_{sc}$ subcarriers allocated to each one. Also, $\sum_{m=1}^{N_{sc}}\sum_{n=1}^{N_{sc}}\Pi_{m,n}(\boldsymbol{\alpha},\hat{P}_{\rm S_3}^{m^\star},\hat{P}_{\rm R_1}^{n^\star},\hat{P}_{\rm R_2}^{n'^\star})$ is a linear combination of $\Delta\sum_{m=1}^{N_{sc}}\sum_{n=1}^{N_{sc}}\Pi_{m,n}(\boldsymbol{\alpha},\hat{P}_{\rm S_1}^{m^\star},\hat{P}_{\rm R_1}^{n^\star},\hat{P}_{\rm R_2}^{n'^\star})+(1-\Delta)\sum_{m=1}^{N_{sc}}\sum_{n=1}^{N_{sc}}\Pi_{m,n}(\boldsymbol{\alpha},\hat{P}_{\rm S_2}^{m^\star},\hat{P}_{\rm R_1}^{n^\star},\hat{P}_{\rm R_2}^{n'^\star})$. Hence, we can directly say the constraints forms linear combinations within themselves. Therefore, we can say that the time-sharing condition is satisfied by (**OP3**). Furthermore, for a given Q, the $\Upsilon(Q)$ is a concave function and the duality gap plummets to zero. Hence proved.

APPENDIX D
PROOF OF PROPOSITION 3

Let us define

$$\mathcal{G}(\Psi(l))=\hat{\mathcal{R}}_T\Big(\boldsymbol{\alpha}^\star(l),\hat{\boldsymbol{P}}_{\rm S}^\star(l),\hat{\boldsymbol{P}}_{\rm R}^\star(l),\hat{\boldsymbol{\Phi}}^\star(l),\hat{\boldsymbol{\Omega}}^\star(l),\hat{\boldsymbol{\Lambda}}^\star(l)\Big)$$
$$-\ \Psi(l)\hat{\mathcal{P}}_T\Big(\hat{\boldsymbol{P}}_{\rm S}^\star(l),\hat{\boldsymbol{P}}_{\rm R}^\star(l),\hat{\boldsymbol{\Phi}}^\star(l),\hat{\boldsymbol{\Omega}}^\star(l),\hat{\boldsymbol{\Lambda}}^\star(l)\Big). \quad \text{(D.1)}$$

Directly following from the iterative algorithm, the new penalty $\Psi(l)$ is updated after the $(l-1)^{\rm th}$ iteration. Therefore, we have (D.2), as shown at the top of this page. Using the definition of $\Psi(l+1)$ in (43), we get (D.3), as shown at the top of this page page. As, $\hat{\mathcal{P}}_T(\hat{\boldsymbol{P}}_{\rm S}^\star(l),\hat{\boldsymbol{P}}_{\rm R}^\star(l),\hat{\boldsymbol{\Phi}}^\star(l),\hat{\boldsymbol{\Omega}}^\star(l),\hat{\boldsymbol{\Lambda}}^\star(l))\geq 0$, always holds true, therefore $\Psi(l+1)\geq\Psi(l)$.

To prove the second part, we use contradiction method. Since $\Psi(l)$ is monotonically increasing and bounded, the sequence $\{\Psi(l)\}$ gets converged. Let us assume $\overrightarrow{\Psi}$ as the convergence point for the sequence, i.e., $\Psi(l)=\Psi(l+1)=\overrightarrow{\Psi}$, but the optimal penalty is not $\overrightarrow{\Psi}$, then the balance equation should not hold true, $\hat{\mathcal{R}}_T(\boldsymbol{\alpha}^\star(l),\hat{\boldsymbol{P}}_{\rm S}^\star(l),\hat{\boldsymbol{P}}_{\rm R}^\star(l),\hat{\boldsymbol{\Phi}}^\star(l),\hat{\boldsymbol{\Omega}}^\star(l),\hat{\boldsymbol{\Lambda}}^\star(l))-\Psi(l)\hat{\mathcal{P}}_T(\hat{\boldsymbol{P}}_{\rm S}^\star(l),\hat{\boldsymbol{P}}_{\rm R}^\star(l),\hat{\boldsymbol{\Phi}}^\star(l),\hat{\boldsymbol{\Omega}}^\star(l),\hat{\boldsymbol{\Lambda}}^\star(l))\neq 0$, therefore using (43), we get

$$\Psi(l)\neq\frac{\hat{\mathcal{R}}_T\Big(\boldsymbol{\alpha},\hat{\boldsymbol{P}}_{\rm S}^\star(l),\hat{\boldsymbol{P}}_{\rm R}^\star(l),\hat{\boldsymbol{\Phi}}^\star(l),\hat{\boldsymbol{\Omega}}^\star(l),\hat{\boldsymbol{\Lambda}}^\star(l)\Big)}{\hat{\mathcal{P}}_T\Big(\hat{\boldsymbol{P}}_{\rm S}^\star(l),\hat{\boldsymbol{P}}_{\rm R}^\star(l),\hat{\boldsymbol{\Phi}}^\star(l),\hat{\boldsymbol{\Omega}}^\star(l),\hat{\boldsymbol{\Lambda}}^\star(l)\Big)}$$
$$=\Psi(l+1), \quad \text{(D.4)}$$

this directly contradicts our assertion of $\Psi(l)=\Psi(l+1)$. Hence when the sequence $\{\Psi(l)\}$ has converged, the penalty at the converging point is the optimal penalty, i.e., $\Psi^\star=\lim_{l\to\infty}\Psi(l)$, satisfying the balance equation. Hence proved.

REFERENCES

[1] E. Gelenbe and Y. Caseau, "The impact of information technology on energy consumption and carbon emissions," *ACM Ubiquity*, vol. 2015, pp. 1–15, Jun. 2015.

[2] K. Singh, M.-L. Ku, J.-C. Lin, and T. Ratnarajah, "Toward optimal power control and transfer for energy harvesting amplify-and-forward relay networks," *IEEE Trans. Wireless Commun.*, vol. 17, no. 8, pp. 4971–4986, Aug. 2018.

[3] I. Ahmed, A. Ikhlef, R. Schober, and R. K. Mallik, "Power allocation for conventional and buffer-aided link adaptive relaying systems with energy harvesting nodes," *IEEE Trans. Wireless Commun.*, vol. 13, no. 3, pp. 1182–1195, Mar. 2014.

[4] L. R. Varshney, "Transporting information and energy simultaneously," in *Proc. IEEE Int. Symp. Inf. Theory*, Toronto, ON, Canada, Jul. 2008, pp. 1612–1616.

[5] X. Zhou, R. Zhang, and C. K. Ho, "Wireless information and power transfer: Architecture design and rate-energy tradeoff," *IEEE Trans. Commun.*, vol. 61, no. 11, pp. 4754–4767, Nov. 2013.

[6] A. A. Nasir, X. Zhou, S. Durrani, and R. A. Kennedy, "Relaying protocols for wireless energy harvesting and information processing," *IEEE Trans. Wireless Commun.*, vol. 12, no. 7, pp. 3622–3636, Jul. 2013.

[7] K. Singh, A. Gupta, and T. Ratnarajah, "QoS-driven energy-efficient resource allocation in multiuser amplify-and-forward relay networks," *IEEE Trans. Signal Inf. Process. Netw.*, vol. 3, no. 4, pp. 771–786, Dec. 2017.

[8] K. Singh, A. Gupta, and T. Ratnarajah, "QoS-driven resource allocation and EE-balancing for multiuser two-way amplify-and-forward relay networks," *IEEE Trans. Wireless Commun.*, vol. 16, no. 5, pp. 3189–3204, May 2017.
[9] S. Modem and S. Prakriya, "Optimization of links with a battery-assisted time-switching wireless energy harvesting relay," *IEEE Syst. J.*, vol. 12, no. 4, pp. 3044–3051, Dec. 2018.
[10] H. Ding, X. Wang, D. B. da Costa, Y. Chen, and F. Gong, "Adaptive time-switching based energy harvesting relaying protocols," *IEEE Trans. Commun.*, vol. 65, no. 7, pp. 2821–2837, Jul. 2017.
[11] T. P. Do, I. Song, and Y. H. Kim, "Simultaneous wireless transfer of power and information in a decode-and-forward two-way relaying network," *IEEE Trans. Wireless Commun.*, vol. 16, no. 3, pp. 1579–1592, Mar. 2017.
[12] D. Sui, F. Hu, W. Zhou, M. Shao, and M. Chen, "Relay selection for radio frequency energy-harvesting wireless body area network with buffer," *IEEE Internet Things J.*, vol. 5, no. 2, pp. 1100–1107, Apr. 2018.
[13] Y. Gu, H. Chen, Y. Li, Y.-C. Liang, and B. Vucetic, "Distributed multi-relay selection in accumulate-then-forward energy harvesting relay networks," *IEEE Trans. Green Commun. Netw.*, vol. 2, no. 1, pp. 74–86, Mar. 2018.
[14] A. Alsharoa, H. Ghazzai, A. E. Kamal, and A. Kadri, "Optimization of a power splitting protocol for two-way multiple energy harvesting relay system," *IEEE Trans. Green Commun. Netw.*, vol. 1, no. 4, pp. 444–457, Dec. 2017.
[15] S. Guo and X. Zhou, "Energy-efficient design in RF energy harvesting relay networks," in *Proc. IEEE GLOBECOM*, San Diego, CA, USA, Dec. 2015, pp. 1–6.
[16] Q. Li, Q. Zhang, and J. Qin, "Secure relay beamforming for SWIPT in amplify-and-forward two-way relay networks," *IEEE Trans. Veh. Technol.*, vol. 65, no. 11, pp. 9006–9019, Nov. 2016.
[17] Q. Wu, M. Tao, D. W. K. Ng, W. Chen, and R. Schober, "Energy-efficient resource allocation for wireless powered communication networks," *IEEE Trans. Wireless Commun.*, vol. 15, no. 3, pp. 2312–2327, Mar. 2016.
[18] Y. Shen, X. Huang, K. S. Kwak, B. Yang, and S. Wang, "Subcarrier-pairing-based resource optimization for OFDM wireless powered relay transmissions with time switching scheme," *IEEE Trans. Signal Process.*, vol. 65, no. 5, pp. 1130–1145, Mar. 2017.
[19] F. Wang, S. Guo, B. Xiao, Y. Yang, and X. Zhang, "Resource allocation and admission control for an energy harvesting cooperative OFDMA network," *IEEE Trans. Veh. Technol.*, vol. 67, no. 5, pp. 4071–4086, May 2018.
[20] J. Petit, F. Schaub, M. Feiri, and F. Kargl, "Pseudonym schemes in vehicular networks: A survey," *IEEE Commun. Surveys Tuts.*, vol. 17, no. 1, pp. 228–255, 1st Quart., 2015.
[21] X. Shen, X. Cheng, R. Zhang, B. Jiao, and Y. Yang, "Distributed congestion control approaches for the IEEE 802.11p vehicular networks," *IEEE Intell. Transp. Syst. Mag.*, vol. 5, no. 4, pp. 50–61, Dec. 2013.
[22] Z. Zhang, K. Long, J. Wang, and F. Dressler, "On swarm intelligence inspired self-organized networking: Its bionic mechanisms, designing principles and optimization approaches," *IEEE Commun. Surveys Tuts.*, vol. 16, no. 1, pp. 513–537, 1st Quart., 2014.
[23] F. Chen, W. Su, S. Batalama, and J. D. Matyjas, "Joint power optimization for multi-source multi-destination relay networks," *IEEE Trans. Signal Process.*, vol. 59, no. 5, pp. 2370–2381, May 2011.
[24] M. W. Baidas and A. B. MacKenzie, "An auction mechanism for power allocation in multi-source multi-relay cooperative wireless networks," *IEEE Trans. Wireless Commun.*, vol. 11, no. 9, pp. 3250–3260, Sep. 2012.
[25] *Further Advancement for E-UTRA Physical Layer Aspects (Release 9) (V9.0.0)*, document TR 36.819, 3GPP, Sophia Antipolis, France, Mar. 2010.
[26] S. Boyd and L. Vandenberghe, *Convex Optimization*. Cambridge, U.K.: Cambridge Univ. Press, 2004.
[27] W. Dinkelbach, "On nonlinear fractional programming," *Manag. Sci.*, vol. 13, no. 7, pp. 492–498, Mar. 1967.
[28] V. Raghunathan, S. Ganreiwal, and M. Srivastava, "Emerging techniques for long lived wireless sensor networks," *IEEE Commun. Mag.*, vol. 44, no. 4, pp. 108–114, Apr. 2006.
[29] R. Zhang and C. K. Ho, "MIMO broadcasting for simultaneous wireless information and power transfer," *IEEE Trans. Wireless Commun.*, vol. 12, no. 5, pp. 1989–2001, May 2013.
[30] W. Yu and R. Lui, "Dual methods for nonconvex spectrum optimization of multicarrier systems," *IEEE Trans. Commun.*, vol. 54, no. 7, pp. 1310–1322, Jul. 2006.
[31] A. Sard, *Linear Approximation*. Providence, RI, USA: AMS, 1963.
[32] H. W. Kuhn, "The Hungarian method for the assignment problem," in *50 Years Integer Programming 1958–2008*. Heidelberg, Germany: Springer, 2010, pp. 29–47.
[33] K. Singh, A. Gupta, T. Ratnarajah, and M.-L. Ku, "A general approach toward green resource allocation in relay-assisted multiuser communication networks," *IEEE Trans. Wireless Commun.*, vol. 17, no. 2, pp. 848–862, Feb. 2018.
[34] V. Singh and H. Ochiai, "An efficient time switching protocol with adaptive power splitting for wireless energy harvesting relay networks," in *Proc. IEEE VTC Spring*, Sydney, NSW, Australia, Jun. 2017, pp. 1–5.
[35] S. O. Krumke, *Integer Programming: Polyhedra and Algorithms*, Technische Universität Kaiserslautern, Kaiserslautern, Germany, Jan. 4, 2006.
[36] P.-H. Huang, Y. Gai, B. Krishnamachari, and A. Sridharan, "Subcarrier allocation in multiuser OFDM systems: Complexity and approximability," in *Proc. IEEE WCNC*, Sydney, NSW, Australia, Apr. 2010, pp. 1–6.

Ankit Gupta received the B.Tech. degree in electronics and communication engineering from Guru Gobind Singh Indraprastha University, New Delhi, India, in 2015. He is currently pursuing the Ph.D. degree in signal processing and communication engineering with Heriot-Watt University. He was with Aricent Technologies, Ltd., (Holdings), Gurugram, India, until 2017. His current research interests include 5G, cooperative communications, multiple-input multiple-output networks, nonorthogonal multiple access techniques, and optimization methods in signal processing and communications.

Keshav Singh (S'12–M'16) received the M.Tech. degree in computer science from Devi Ahilya Vishwavidyalaya, Indore, India, in 2006, the M.Sc. degree in information and telecommunications technologies from AIT, Greece, in 2009, and the Ph.D. degree in communication engineering from National Central University, Taiwan, in 2015. Since 2016, he has been with IDCOM, University of Edinburgh. His research interests are in the areas of resource allocation, full-duplex radio, IoT, cooperative and energy harvesting networks, nonorthogonal multiple access, and machine learning techniques for caching in future wireless networks.

Mathini Sellathurai (S'95–M'01–SM'06) is currently a Professor in signal processing for communications and intelligent systems with Heriot-Watt University. Her research interests include signal processing, pattern recognition, machine learning and artificial intelligence, and future wireless networks. She was a recipient of the IEEE Communication Society Fred W. Ellersick Best Paper Award in 2005, the Industry Canada Public Service Awards in 2005, and the Best Ph.D. thesis Award (Silver Medal) from NSERC Canada in 2002. She has been an Editor for IEEE TRANSACTIONS ON SIGNAL PROCESSING since 2009. She is the General Co-Chair of IEEE SPAWC 2016, Edinburgh, U.K. She is also a member for IEEE SPCOM Technical Strategy Committee.